

**T-PM-Po29** THE ACTIVITY OF RESTRICTION ENDONUCLEASES ON UV-IRRADIATED DNA. R. K. Hall and L. L. Larcom, Departments of Physics and Microbiology, Clemson University, Clemson, SC 29631.

The recognition sequences of some restriction endonucleases contain two adjacent thymine bases and thus potential thymine dimer sites. To determine whether thymine dimers would interfere with the activity of EcoRI or HindIII we irradiated phenol extracted DNA from the *Bacillus subtilis* phage SPPI with different doses of 254 nm radiation. Unirradiated DNA and irradiated DNA were digested separately and the resulting fragments were electrophoresed on 1% agarose gels and stained with ethidium bromide. The patterns obtained revealed 14 new bands for the EcoRI digested irradiated DNA and 8 new bands for the HindIII digested irradiated DNA. As the dose of UV was increased, the amount of material observed in fragments normally obtained with unirradiated DNA decreased with a concomitant increase in the amount present in the new bands. The results are consistent with the interpretation that dimerization of thymines in the recognition sites makes these sites unsuitable for cleavage by the enzymes.

This investigation was supported in part by Grant Number CA21479, awarded by the National Cancer Institute, DHHS.

**T-PM-Po30** STATISTICAL CONFORMATIONAL PROBES OF THE POLYNUCLEOTIDE HELIX-COIL TRANSITION.

N.L. Marky and W.K. Olson, Department of Chemistry, Rutgers University, New Brunswick, N.J. 08903

Conformational details of the helix-to-coil transition of a polynucleotide chain can be monitored in terms of the two virtual bonds connecting phosphorus and 4'-carbon atoms in each nucleotide repeating residue. According to simple hard-core arguments, the interactions of adjacent bases introduce "long-range" angular correlations that restrict the motions of successive C-C and O-P bond rotations at low temperatures. With increase of temperature, however, the torsions vary nearly independently over the large regions of conformation space. Both the root-mean-square end-to-end separation  $\langle r^2 \rangle^{1/2}$ , and the persistence vector of the chain  $p = \langle r \rangle$  decrease in magnitude upon such changes. Configurational averages of Cartesian tensors formed from the displacement vector  $p = r - p$  indicate that the three-dimensional spatial distributions and the loop closure tendencies of the polynucleotide chain respond as well to temperature effects.

(Supported by N.I.H. grants GM-20861 and CA-25981 and PRF grant AC-11586).

**T-PM-Po31** INTERPRETING CIRCULAR DICHROISM SPECTRA FOR STACKING INTERACTIONS. Gary C. Causley, Paul W. Staskus and W. Curtis Johnson, Jr., Department of Biochemistry and Biophysics, Oregon State University, Corvallis, OR 97331.

Circular dichroism spectra of stacked homopolymers have been described by many workers as either conservative or nonconservative depending upon the degree of gaussian and first derivative shape in the curve. Present theory suggests that the conservative (derivative) shape is related to the amount of stacking in nucleic acid polymers and is the result of strong coupling of transition moments on adjacent bases. We have re-examined this feature in stacked dimers and polymers of adenosine and cytidine as a function of temperature. A variety of numerical techniques have been employed to deconvolute the spectra into the components which are related to conformational and configurational changes as the structures are melted. We use a variation of the technique of Powell and Gratzer<sup>1</sup> on parameters related to stacking to obtain accurate thermodynamic data, as well as the stacking contribution to circular dichroism curves at temperature extrema. The results show that, at the extrema, stacking terms of the dimers and polymers are nearly identical. This result is unexpected in the light of present theory. We also show that as single stranded homopolymers are melted, the large non-cooperative changes in the circular dichroism curves are accompanied by smaller cooperative changes. This is thought to be the result of configurational variations in the monomers. (This work was supported by NSF grant PCM 80-21210).

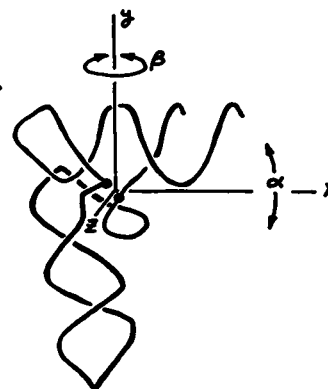
<sup>1</sup>Powell, Janet T., Richards, E. G. and Gratzer, W. B. (1972) *Biopolymers* 11, 235-250.

**T-PM-Po32** STEREOCHEMISTRY OF 2'-5' LINKED OLIGONUCLEOTIDES: CRYSTAL STRUCTURE OF A2'p5'C, A DINUCLEOSIDE MONOPHOSPHATE WITH A NOVEL PHOSPHODIESTER LINKAGE. R. Parthasarathy, Manju Malik and Susan M. Fridey, Center for Crystallographic Research, Roswell Park Memorial Institute, Buffalo, New York 14263, USA.

DNA, RNA and tRNA contain 3'-5' phosphodiester bonds, but "two-five A" - pppA2'p5'A2'p5'A, the messenger induced in interferon treated cells, contains 2'-5' links. In order to understand why do DNA and RNA have the 3'-5' link and to delineate the stereochemistry of the 2'-5' links, we carried out an accurate crystallographic analysis of A2'p5'C crystals obtained in the free acid form at pH 4.5. Crystals are orthorhombic,  $a = 8.631(1)$ ,  $b = 18.099(1)$ ,  $c = 16.101(1)$  Å,  $P2_12_12_1$ ,  $Z = 4$ , 5998 reflections (both hkl and  $\bar{h}\bar{k}\bar{l}$ ),  $R = 0.03$ . The conformation of A and C are, respectively, syn, C2'-endo,  $g^+$  and anti, C3'-endo C2'-exo,  $g^+$ ; the phosphodiester conformation is ( $g^-, g^-$ ). There is no intramolecular base stacking, but A stacks on top of the O(4') of C. Our reexamination of the crystal structure of A2'p5'U also shows such A...O(4') of U stacking, though A has anti conformation in this structure. Stacking of the O(4') of the nucleoside sequentially next to a purine, whether the purine is syn or anti, is an important feature in 2'-5' purine-pyrimidine sequences. But in 3'-5' nucleotides, model building studies show that a syn purine can not stack on top of the O(4') of the next nucleoside (due to sterical reasons) but can stack on the O(4') of the previous nucleoside (as in the Z-DNA structure). This conformational difference between 2'-5' and 3'-5' links arises because the 2'-link orients the backbone inwards towards the base unlike the 3'- and 5'-links that orient the backbone away from the bases. (Supported by USPHS NIH Grant GM 24864.)

**T-PM-Po33** CONFORMATIONAL ENERGY MAP FOR INTRAMOLECULAR BENDING IN PHENYLALANINE TRANSFER RNA. Stephen C. Harvey<sup>a</sup> and J. Andrew McCammon<sup>b</sup>, (a) Biophysics Section, Department of Biomathematics, University of Alabama in Birmingham, Birmingham, AL 35294, and (b) Department of Chemistry, University of Houston, Houston, TX 77004.

We have established a computer-based model for tRNA<sup>Phe</sup> for the examination of motions within the molecule. The model uses a set of empirical energy functions to calculate the energy of any specified conformation, and it can relax stresses which arise from bending the molecule, allowing the determination of local minimum energy structures. In a preliminary study (Harvey and McCammon, *Nature*, in press), we reported the dependence of energy on each of two independent degrees of freedom, the motions of bending ( $\alpha$ ) and swinging ( $\beta$ ) about a swivel located between P8 and P49 (dark points). We have extended that work with an examination of motions combining bending and swinging, determining a conformational energy map  $E(\alpha, \beta)$ , and we have found little steric resistance to large motions. The arms move through angles as large as  $30^\circ$  at an energetic cost of only a few kcal per mol, suggesting that flexibility is modulated by interactions with other macromolecules and by solvent conditions, especially pH, ionic strength, and the concentration of polyvalent cations. (This work was supported in part by the National Science Foundation.)



**T-PM-Po34** NMR STUDIES OF THE INTERACTION BETWEEN BIS-INTERCALATORS AND SYNTHETIC DNA.

N. Assa-Munt, W.A. Denny\* and D.R. Kearns, Department of Chemistry, University of California-San Diego, La Jolla, California, \*Cancer Chemotherapy Research Laboratory, University of Auckland, School of Medicine, Private Bag, Auckland, New Zealand.

A well defined, synthetic (AT)<sub>5</sub> DNA decamer has been used to study by NMR the mode of binding and kinetics of binding of bis-amino acridine and bis-methidium spermine to DNA. Important resonances in the lowfield region (10-15 ppm), which arise from the imino protons in Watson-Crick base pairs, have been monitored as increasing amounts of the mono- and bis-analogues of the above mentioned drugs are added. In the case of the mono-analogues, a single new peak arises at  $\sim 12.5$  ppm, corresponding to  $\sim 20\%$  of the total intensity at 1:1 drug/decamer. When the bis-analogues are added, two distinct new peaks appear, which may indicate that the neighboring A-T base pairs are affected differently. The fact that the new shifted resonances at 1:1 drug/decamer correspond to 40% of the total intensity is taken as an indication that both chromophores in the bis-analogues are intercalated. Relaxation studies of these drug-DNA complexes in H<sub>2</sub>O, using the time-shared 214 and the soft pulse method have also been undertaken.

**T-PM-Po35** COMPARATIVE H-1 AND P-31 NMR STUDIES OF NUCLEIC ACID HOMOPOLYMERS CONTAINING DIFFERENT C-2' FURANOSE SUBSTITUENTS. J. L. Alderfer, R. E. Rycyna and R. E. Loomis. Roswell Park Memorial Institute, Biophysics Department, Buffalo, N. Y. 14263.

Proton NMR spectroscopy reveals base-stacking interactions (from polymerization shifts,  $\Delta\delta p$ ) and furanose conformations (from J values), while P-31 data elucidates phosphate-backbone conformations. Homopolymers of A,I,C, and U(T) containing C2'-H(d), or -OH(r), or -OCH<sub>3</sub>(m) furanose substituents are studied.  $\Delta\delta p$  values indicate stacking orders of purine polymers (Biochem.(1975), 13,1615; Biophys.J.(1975)15,29a) are d>r>m, and of cytosine m>r>d.  $\Delta\delta p$  values of dT, rU and mU are (30°, ppm): H6(-0.07,-0.11,-0.10), H5 or CH<sub>3</sub>(-0.06,-0.04,-0.07), H1'(-0.12,-0.02,-0.01), suggesting a stacking order of mU>rU>dT. J(H1',H2') of mU, rU and dT is 4.5, 5.8, and 6.7Hz. This J of mU at low temperature is similar to monomer but increases with increasing temperature, rU is larger than monomer and temperature independent, and dT is identical to monomer and temperature independent. This data indicates the furanose conformation of mU shifts from C3'- to C2'-endo forms with increasing temperature. P-31 chemical shifts ( $\delta$ ,ppm,trimethylphosphate)(30°, 60°) are: dA,rA,mA-(-4.56,-3.97,-4.28 and -4.33,-3.72,-4.06), dI,rI,mI(-4.34,-3.70,-4.09 and -4.14,-3.55,-3.93), dC,rC,mC(-4.05,-4.23,-4.53 and -3.93,-4.00,-4.38), dT,rU,mU(-4.20,-3.81,-4.30 and -4.05,-3.64,-4.11). Upfield shifts suggest increasing g,g conformations of  $\omega,\omega'$ (O5'-P5',O3'-P3')(facilitates base-stacking interaction). Relative shieldings of dA>rA, dI>rI, rC>dC, mC>rC and mU>rU are consistent with  $\Delta\delta p$  and J(H1',H2') values. Relative shieldings of mA>rA, mI>rI, and dT>rU are not consistent with  $\Delta\delta p$  and J values. Comparison with model compounds indicates these P-31 chemical shift effects manifested here are not primarily due to conformational differences ( $\omega,\omega'$ ), but to differing anisotropies of the C-2' substituents.

**T-PM-Po36** X-RAY CONFORMATIONAL STUDY OF THE CRICK-WATSON HELIX IN SOLUTION. V. Grassian and G.W. Brady, Rensselaer Polytechnic Institute, Troy, N.Y. 12121 and N.Y. State Department of Health, Albany, N.Y. 12201

Earlier x-ray studies on dissolved linear DNA molecules (1,2) were interpreted on the assumption that the molecules scattered as rigid rods. Improvement in equipment and advances in theory of the scattering from randomly oriented helices prompted us into a reinvestigation action of this problem. Careful measurements were made on the scattering from both linear calf thymus DNA and from circular plasmid COP608 superhelical DNA. Contrary to the earlier work we find that the scattering patterns show a helical character, with maxima corresponding to those of a helix with pitch angle of 62°, close to that of the C-W helix. The patterns for both types of DNA, although similar, show a 5% displacement of the maximum in the superhelical form, just that expected when the C-W helix is superimposed on a superhelix axis. Introduction of intercalators (PtTS) causes a progressive extension of the helix, as shown by a shift to smaller angles and a fading out of the maximum. In the concentration range of 40 mg/ml interference peaks develop, the result of an apparent stacking of the chains, with an interchain distance of ~ 35 Å. Our experiments thus indicate that the rigid rod approximation for the secondary structure of DNA molecules is not an appropriate one.

V. Luzzati, F. Masson, A. Mathis and P. Saludjian (1967). Biopolymers 5, 491-508.  
S. Bram and W.W. Beeman (1971). J. Mol. Biol. 55, 311-324.

**T-PM-Po37** COUNTERION CONDENSATION OF DNA STUDIED BY ELECTROPHORETIC LIGHT SCATTERING. Wei S. Yen and B. R. Ware, Department of Chemistry, Syracuse University, Syracuse, New York 13210.

The condensation of counterions onto a linear polyelectrolyte has been treated from considerations of electrostatic energetics in a series of papers by Manning. This simple theory has been remarkably successful in comparisons with experimental data, but there is a paucity of data for which direct comparisons are straightforward. We have performed a series of experiments on synthetic polynucleotides, bacteriophage  $\lambda$  DNA, and chromosomal DNA using the technique of electrophoretic light scattering. Condensation replacement experiments were performed by titrating DNA solutions in low uni-univalent salt buffers with multivalent ions such as Mg<sup>+2</sup> and spermine (+3). Increased counterion condensation was observed through the reduction of the electrophoretic mobility of the polyelectrolyte. After a certain fraction of the charge had been neutralized, the polyelectrolyte was observed, through an increased ELS line broadening, to collapse in conformation, a phenomenon also referred to by some authors as condensation. The critical parameter for prediction of condensation and collapse is the multi-valent to uni-valent counterion concentration; no dependence on polyelectrolyte concentration is observed. Our observations are consistent with the Manning theory for counterion concentration if the polyelectrolyte volume parameter is treated as an adjustable parameter, and reasonable values of the volume parameter are obtained for an optimized fit to the data. (This work was supported by NIH Grant No. GM27633 and by a grant from the Petroleum Research Foundation, administered by the American Chemical Society.)

**T-PM-Po38** NMR AND BIOCHEMICAL STUDIES OF POLY(5-FLUOROURIDYLIC) ACID. Ronald E. Loomis, Geraldine L. Hazel, and James L. Alderfer, Department of Biophysics, Roswell Park Memorial Institute, Buffalo, New York 14263.

A comparative study is made of the chemical shifts, coupling constants, polymerization shifts, and biochemical behavior of poly(FU) and poly(U). Within a pH range of 6.0-9.5 the following coupling constants (Hz) for poly(FU) and FUrd (underlined) remain constant:  $^3J_{H1',H2'}$  (6.1±0.1, 4.4±0.1),  $^5J_{H1',F5}$  (1.5±0.4, 1.5±0.2),  $^3J_{H6',F5}$  (6.2±0.1, 6.4±0.1). The  $^3J_{H1',H2'}$  of poly(U) and Urd is 5.8±0.1 (pH 6.0-9.5) and 4.5±0.1 (pH 7.0), respectively. Sigmoidal curves of  $\delta$  vs pH characterize the H6 plot of both poly(FU) (pKa = 8.1) and FUrd (pKa = 7.8). The H1' plot is also sigmoidal for poly(FU), but linear for FUrd. Proton polymerization shifts,  $\Delta\delta_p = \delta(\text{polymer}) - \delta(\text{monomer})$  at pH 6.0 and 30° for poly(U) and poly(FU) (underlined) are: H1' (-0.015, -0.010), H6 (-0.106, -0.057), H5 (-0.043). Temperature dependent titration curves ( $\delta$  vs pH) of poly(FU), poly(U<sub>19</sub>,FU), poly(C<sub>14</sub>,FU), and FUrd are obtained utilizing  $^{19}\text{F}$ -NMR spectroscopy. Enzymatic degradation as measured by UV hyperchromicity (at 50% maximum) with micrococcal nuclease (24°, pH 8.8) is 8 minutes for poly(U) and 27 minutes for poly(FU). Similarly, snake venom phosphodiesterase (37°, pH 8.9) degrades poly(U) approximately three times faster than poly(FU). These collective data indicate: (1) poly(FU) changes sugar-base torsion angle with pH, (2) poly(FU) is less base-stacked than poly(U), (3) population of C3'-endo furanose conformation is FUrd>Urd>poly(U)>poly(FU), (4) the pKa(N3-H) has relative magnitudes of poly(FU)>poly(U<sub>19</sub>,FU)>FUrd, (5) hydrolytic stability of poly(FU) is greater than poly(U) using micrococcal nuclease and snake venom phosphodiesterase. Supported by NIH Grant CA-25438.

**T-PM-Po39** NMR AND EQUILIBRIUM DIALYSIS STUDIES OF CATION BINDING TO DNA. W. H. Braunlin, M. L. Bleam, T. J. Strick and M. T. Record, Jr., Department of Chemistry, University of Wisconsin, Madison, Wisconsin 53706.

We have monitored by two complementary techniques the competitive binding of such oligocations as  $\text{Mg}^{2+}$ , putrescine, spermidine, spermine and  $\text{Co}(\text{NH}_3)_6^{3+}$  to DNA. Equilibrium dialysis has been employed to measure thermodynamic binding, while  $^{23}\text{Na}$  and  $^{59}\text{Co}$  NMR have provided information on shorter range interactions. The NMR measurements allow bounds to be placed on the extent of  $\text{Na}^+$  binding to DNA in the limit of no added multivalent competitor. The limiting ratio of bound sodium to phosphate is found to be between 0.2 and 0.6, depending on the model used to interpret the data. The equilibrium dialysis measurements yield observed binding constants ( $K_{\text{obs}}$ ) whose salt-dependence is qualitatively consistent with theoretical predictions for the binding of charged ligands to a rod-like polyanion. We also observe an insignificant variation in  $K_{\text{obs}}$  for spermine and spermidine over the temperature range of 4° to 37°C, as expected for a predominantly electrostatic binding reaction. Combining the two types of measurements provides a quantitative test for the predictions of the two major competing models for cation binding to DNA: the two variable theory of Manning and the Poisson-Boltzmann theory.

**T-PM-Po40** SOLUTION PROPERTIES OF Z-FORM DNA. D.C.Rau and E.Charney, Laboratory of Chemical Physics,NIADDK, NIH, Bethesda,Md. 20205, and Holly Ho Chen, Dept. of Chem George Mason Univ., Fairfax, Va. 22030 (Intr. by W.A. Hagins)

Recently Behe and Felsenfeld (Proc. Natl. Acad. Sci. 78,1619,1981) reported that synthetic poly(G-m<sup>5</sup>C) undergoes a transition from a B-form circular dichroic spectrum to one that is characteristic of left handed Z-form DNA, at very low salt concentrations with very small amounts of added cobalt hexamine (less than 1  $\text{Co}(\text{NH}_3)_6^{3+}$  per 5 DNA phosphates). In an effort to compare solution properties of these different forms with x-ray structures, using transient electric dichroism we have measured rotational diffusion coefficients of fairly monodisperse, 145 bp poly(G-m<sup>5</sup>C) samples obtained by nucleosome trimming. At 2°C, the rotational relaxation time of the B-form is 4.2±0.3  $\mu\text{sec}$ . On adding  $\text{Co}(\text{NH}_3)_6^{3+}$ , this increases to 5.4±0.3  $\mu\text{sec}$ . These times are independent of the ionic strength in the range 0.2 to 2.5 mM  $\text{Na}^+$ , suggesting that these small fragments are essentially rods. Applying a number of hydrodynamic theories to the data, the increase in rotational times corresponds to a 10% lengthening of poly(G-m<sup>5</sup>C) between the B-form and the CD defined Z structure. This change is consistent with the increase in the axial rise per base pair (from 3.4 Å to 3.6-3.8 Å) determined by fiber diffraction.

**T-PM-Po41** SPERMIDINE-DNA TORUS STRUCTURE: EVIDENCE FOR CONTINUOUS CIRCUMFERENTIAL DNA WINDING.

K.A. Marx, T.C. Reynolds & G.C. Ruben, Dept. of Chemistry, Dartmouth College & Dept. of Pathology & Biology, Dartmouth Medical School, Hanover, N.H.

Polyamines are major, ionic constituents of virus and bacteriophage heads. Using spermidine we have condensed Calf Thymus,  $\lambda$ , E. Coli. and  $\phi$ X-174 DNA to virus-sized, toroidal shaped structures. Two major pieces of experimental evidence strongly support a continuous circumferential winding model for DNA organization in toruses. 1) Freeze-fracture EM has revealed surface Pt/C decoration consistent with DNA lying circumferentially on the torus surface. 2) Micrococcal nuclease digestion of spermidine-condensed linear DNAs yielded an arithmetic series of DNA fragment lengths in gels. The zero-digestion time extrapolated monomer DNA lengths vary between 800 and 1000 bp depending on the DNA. This result is consistent with a model for torus formation from continuous circumferentially wound DNA in which the monomer DNA length winds exactly one torus circumference. The arithmetic DNA band series can be generated from a localized torus cleavage model by micrococcal nuclease. When nicked, circular  $\phi$ X-174 RF II DNA was spermidine-condensed and micrococcal nuclease digested, 7 discrete bands were found to form an arithmetic series based on a  $780 \pm 50$  bp, zero-digestion-time length monomer. This small (5386 bp), monodisperse DNA must undergo 7 (5386 bp/780 bp) circumferential windings in order to make a uniform torus. This result is inconsistent topologically with torus formation by blunt-end-rod-fusion and strongly supports continuous circumferential DNA wrapping to form toruses. These data support the co-axial spool model for DNA organization in bacteriophage. The authors acknowledge Res. Corp. #8859, NIH GM 25886-02, NIH AI17586-01 BBCA, & Biomed. Res. Sup. RR-05392 (KAM) & Norris Cotton Cancer C. #CA23108 NCI (GCR).

**T-PM-Po42** SCANNING TRANSMISSION ELECTRON MICROSCOPY OF THE ARRANGEMENT OF NUCLEOSOMES IN CHROMATIN

IN 80mM NaCl. R.P. Hjelm, Jr. and C.A. Gedye, Medicinal Chemistry, University of Illinois Medical Center, Chicago, Illinois, 60680.

Long fragments of chromatin fibers, greater than 150 nucleosomes in length, in 80mM NaCl are mounted for scanning transmission electron microscopy and negatively stained. The fibers, which are about 300 Å in diameter, follow a serpentine path and show frequent knobby protrusions. They are apparently kinked in places and often seem to fold back on themselves. Occasionally, structures are seen which appear to be sections of fiber thrown into a few adjacent helical gyres. Platinum-shadowed specimens viewed in the transmission electron microscope confirm these observations and show that the fibers do not readily collapse. Distinct banding is evident in negatively stained fibers. Often, the bands can be resolved into lines of nucleosomes. In straight segments of fibers the bands and the positions of nucleosomes indicate an organization not unlike a helix with pitch 110 Å proposed from x-ray and earlier electron microscopic studies. Nucleosomes in adjacent helical turns sometimes appear to be stacked directly above one another along the helix axis. More often the nucleosomes seem to be out of register in neighboring gyres, giving rise to steeply pitched striations in the fibers. There is no common angle that the striations take relative to the axis of the fiber. These results suggest that the helical arrangement of nucleosomes in the fiber is variable. This is supported by the observation that the fibers do not have the rigid form which would be the result of a regular helical structure. Some variation in helical organization must be present to accommodate the observed curvature in the fibers. These observations may bear on the organization of the 300 Å fiber in the nucleus where considerable curvature of the fiber may be necessary for dense packing of the fiber.

**T-PM-Po43** METAL CATION CATALYZED  $H_2O_2$  BREAKDOWN TO HYDROXYL FREE RADICAL AND DNA STRAND BREAKAGE

C. A. Lewis and R. A. Floyd, Oklahoma Medical Research Foundation, Oklahoma City, Oklahoma 73104

In this study, 5,5-dimethyl pyrroline-N-oxide (DMPO) was used to trap the hydroxyl radicals produced during the  $Fe^{++}$  or  $Cu^{++}$  catalyzed decomposition of  $H_2O_2$  under a variety of conditions. Results show that the amount of OH spin-trapped was dependent upon a) the oxidation state of the metal cation, b) the chelator used, and c) the buffer used. Studies on the attack of DNA by OH showed that DNA bound  $Fe(II)$  in a manner such that oxidation of the cation in the buffer system was slowed down when  $Fe(II)$  was bound to the DNA. Addition of  $H_2O_2$  to the DNA- $Fe(II)$  system produced OH radicals and resulted in aldehyde formation, indicating DNA strand breakage. Results with individual bases and their mono-, di-, and triphosphate esters indicate that the presence of some bases such as adenosine may cause enhancement of the amount of OH radicals generated. The results obtained are summarized in the table below. Ratio of DMPO hydroxyl adduct in the presence of Tris buffer only (pH 7.4).

	Adenosine	Thymidine	Guanosine	Cytidine
Base	2.3	1.2	ND	1.1
Nucleoside	2.3	1.3	ND	1.2
5'-monophosphate	1.9	1.1	1.0	1.3
5'-diphosphate	1.3	0.8	1.4	1.7
5'-triphosphate	1.8	1.8	1.6	1.9

Mean values for several observations.

**T-PM-Po44** STRUCTURAL STUDIES OF DRUG-NUCLEIC ACID INTERACTIONS: MOLECULAR GEOMETRY OF STACKING INTERACTIONS. Shih-Chung Kao, Christian G. Reinhardt and Chun-che Tsai, Department of Chemistry, Kent State University, Kent, Ohio 44242.

A generalized stereochemical scheme has been developed in our laboratory. This scheme can be used for comparing the stacking patterns between the adjacent base-pairs in double-helical nucleic acids which have defined base sequences. It can also be used for comparing the stacking patterns between adjacent base-pairs within the intercalated drug-nucleic acid structures of various drug-nucleic acid complexes. This scheme uses a set of unified structural parameters to compare the double-helical nucleic acid structure before and after distortion has been induced by binding the nucleic acid to intercalative drugs. This stereochemical scheme, and its associated structural parameters, has been combined with theoretical proton NMR chemical shift change calculations which were derived from both the ring current and the atomic anisotropy contributions of the nucleic acid bases. This has allowed us to quantitatively define certain aspects of the molecular geometry of stacking interactions in solution for several drug-nucleic acid complexes by direct comparison of the experimentally observed and the theoretically calculated drug (or nucleic acid) proton NMR chemical shift changes which are induced by the binding of intercalative drugs to nucleic acids. (Supported by NIH grant GM 24259).

**T-PM-Po45** COOPERATIVITY AND ALLOSTERISM IN THE BINDING OF THE ANTICANCER DRUG DHAQ TO DNA. L.S. Rosenberg and T.R. Krugh, Department of Chemistry, University of Rochester, Rochester, N.Y. 14627.

The interaction of the antineoplastic drug 1,4-dihydroxy-5,8-bis[2-[(2-hydroxyethyl)amino]ethyl]amino-9,10-anthracenedione (DHAQ) with DNAs has been studied by optical titration. In these studies the DHAQ/DNA binding isotherms have been extended to very low values of  $r$  (concentration of bound drug/concentration of polymer). Results indicate that DHAQ binds to DNA in a positive cooperative manner, as evidenced by an initially increasing slope in the Scatchard plots. Factors affecting the conformation of DNA in solution were found to alter the shape and magnitude of the DHAQ/DNA binding isotherm. Raising the ionic strength of the buffer (from 0.2 to 0.6) decreases the initial (increasing) slope in the binding isotherm. Also, raising the temperature (at the ionic strengths studied) diminishes the positive slope observed at low  $r$  values. Neither, the presence of an organic solvent in the buffer (1-nonanol which is used in phase partition analysis) nor a slight change in the pH (6.4 to 7.1) affects the cooperative binding of DHAQ. The shape of the binding isotherm may reflect a drug-induced allosteric change in the solution structure of the DNA. The presence of cooperativity and/or allosteric transitions in the binding of DHAQ by DNA may be an important aspect of its pharmacological activity.

**T-PM-Po46** INTERACTION OF INTERFERON-INDUCING DRUGS WITH NUCLEIC ACIDS: APPLICATIONS OF SOLUTION SPECTROSCOPIC STUDIES TO MOLECULAR CO-CRYSTALLIZATION. Christian G. Reinhardt\*, Daniel G. Flowers and Chun-che Tsai. Department of Chemistry, Kent State University, Kent, OH 44242.

DEAP-Fluoranthene (RMI 9563 DA), a tilorone.HCl derivative, exhibits a diverse range of antitumor, antiviral and interferon-inducing activity. This drug interacts directly with double-helical nucleic acids, possibly by intercalating between adjacent base-pairs of double-stranded DNA. Recent binding studies suggest that Tilorone.HCl (parent compound) may exhibit base specific or preferential binding to alternating Pyr-Pur sequences of double-stranded nucleic acid homopolymers, particularly those containing alternating A-T or T-A sequences (Sturm et. al., Biopolymers, 20, 765 1981.) The binding of the DEAP-fluoranthene derivative to various A,T-containing mononucleotides (dAMP, dTMP), self-complementary deoxydinucleotides (dTpdA, dApdT), tetranucleotides ((dTpdA)<sub>2</sub>, (dApdT)<sub>2</sub>), polynucleotides (poly(dA-dT)) and DNA has been examined by solution spectroscopic techniques. These studies have served to: 1) assess the feasibility of using mono-, di- and tetranucleotide complexes with DEAP-fluoranthene as models for the binding of this drug to DNA; and 2) determine the appropriate nucleic acid fragments, sequences and solution stoichiometry necessary for successful co-crystallization of nucleic-acid-DEAP fluoranthene complexes. The combination of solution spectroscopic studies in conjunction with molecular co-crystallization and X-ray diffraction analyses of single-crystal complexes would help to elucidate the stereochemistry of drug-nucleic acid interactions and the possible mechanisms associated with the pharmacological action of this low molecular weight interferon inducer. (Supported by NIH Grant GM 24259)

\* Current Address: Dept. Chemistry, Rochester Institute of Technology, Rochester, N.Y. 14623

**T-PM-Po47** EPR SOLUTION STUDIES COMPARING THE 3' ENDS OF tRNA<sup>Phe</sup> AND tRNA<sup>Met</sup>, Rita H. Pscheidt and Barbara D. Wells, Department of Chemistry, University of Wisconsin-Milwaukee, Milwaukee, WI 53201.

The crystal structure of *E. Coli* tRNA<sup>Met</sup> (Woo, et al., NATURE 286, 346 (1980)) shows the 3' end of the molecule folded over in a manner which may constrain its motion. This appears to be a large perturbation when compared to the freely rotating 3' end of yeast tRNA<sup>Phe</sup>. Since the suggestion was made that the tRNA<sup>Met</sup> structure might be an artifact of crystallization, solution studies (aqueous buffer, room temperature) were designed to address this question. Nitroxide spin labels were covalently bound to the 3' ends of both molecules. Measurement of the resultant EPR spectra (Tris + 10 mM Mg<sup>++</sup>) indicated different degrees of immobilization; the rotational correlation time of tRNA<sup>Phe</sup> was found to be .57 n sec while that of tRNA<sup>Met</sup> was 1.1 n sec. This would appear to indicate different environments for the 3' ends. Studies of the effect of divalent cations (Mg<sup>++</sup> and Co<sup>++</sup>) are also being followed to further assess the configuration of the 3' termini of these molecules.

**T-PM-Po48** THE BINDING AT HIGH BASE PAIR/BOUND DRUG RATIOS OF SMALL MOLECULES TO DNA: ROLE OF SIDE CHAINS IN THE COOPERATIVE BINDING OF INTERCALATORS TO DNA. Stephen A. Winkle. Department of Chemistry, Rutgers, The State University of New Jersey, New Brunswick, N.J. 08903.

Several antitumor drugs possessing side chains capable of interacting with the DNA helix have been shown to bind with positive cooperativity to DNAs, e.g., actinomycin D (Winkle and Krugh (1981) Nucleic Acids Res. 9, 3175-3186); distamycin (Hogan, Dattagupta and Crothers (1979) Nature 278, 521-524); 1,4-dihydroxy-5,8-bis((2-hydroxyethyl)amino)ethylamino-9,10-anthracenedione (DHAQ) (Winkle, unpublished results). Recent <sup>1</sup>H NMR results suggested that the side chains of DHAQ interact with the DNA (Winkle, unpublished). The results of studies on the role of such side chain-DNA interactions in the cooperativity observed in the binding of molecules possessing side chains to DNA are presented in this paper. The series of side chains was: (aminoethyl)amino; ((aminoethyl)-aminoethyl)amino; (((aminoethyl)aminoethyl)aminoethyl)amino; spermidyl; (((3'-aminopropyl)-piperazyl)propyl)amino; (6'-aminohexyl)amino). The side chains were synthetically added to the 9-position of the chromophore acridine. The equilibrium binding of this series of molecules were studied by optical titration methods and by phase partition studies - with the emphasis on the binding at low r (where cooperativity is most observable). The changes in apparent cooperativity are correlated with the changes in side chain length, side chain stiffness, and the number of potential DNA-binding functional groups (amino groups) on the side chains.

**T-PM-Po49** CONFORMATIONAL PROPERTIES OF TWO RESTRICTION FRAGMENTS FROM THE LACTOSE PROMOTER REGION. J. T. Harrell, S. Abhiraman, and R. M. Wartell, Georgia Institute of Technology, Atlanta, GA 30332.

Raman spectroscopy and circular dichroism were employed to examine two DNA fragments from the transcription initiation region of the *E. coli* lactose operon. One fragment, 144 bp. in length, contains the binding sites for RNA polymerase, the *lac* repressor and the CAP protein. The second fragment, 64 bp. long, contains the CAP binding site and is identical to one end of the 144 bp. DNA. Milligram quantities of the fragments were isolated from plasmids pRMW27 and pRMW30 (Wartell and Reznikoff, *Gene* 9, 307, 1980). Plasmid DNAs were isolated by a modification of previous procedures (Hardies, S. C. and Wells, R. D., *Gene* 7, 1, 1979). In order to optimize *EcoRI* cleavage of large scale preparations standard EtBr - CsCl gradient centrifugation was followed by centrifugation in CsCl. After plasmid cleavage with *EcoRI*, fragments were separated from the cloning vector using selective PEG precipitation and RPC-5 chromatography. Raman spectra of the 144 bp. fragment in 10 mM NaCl and 4.5 M NaCl are similar to spectra of a 95 bp. fragment which contains the operator region but not the CAP binding site (unpublished observations). The low and high salt spectra show some differences but both are indicative of a B conformation. A quantitative comparison between Raman bands of the 144 bp. DNA and other DNAs with varying % G-C content will be presented. The CD spectra of the 64 bp. and the 144 bp. fragments were obtained in 10 mM and 4.5 M NaCl. The low salt spectra of both fragments exhibit positive peaks at approx. 275 nm and negative peaks at approx. 245 nm characteristic of a B conformation. On shifting to high salt the intensities of the peaks change but neither fragment displays an inversion of the peaks. These spectra will be compared with CD spectra of non-promoter fragments.

**T-PM-Po50** SPIN-LATTICE RELAXATION STUDIES OF A DEOXYRIBOSYL DECAMER HELIX, d-(CCAAGCTTGG)<sub>2</sub> - NH RESONANCES AND CH RESONANCES OF THE BASE PROTONS. D.M. Cheng, L.S. Kan, H. Fritzsche, P.S. Miller and P.O.P. Ts'o, Division of Biophysics, The Johns Hopkins University, Baltimore, Md. 21205, and Department of Biophysical Chemistry, Central Institute of Microbiology and Experimental Therapy, Academy of Sciences of the German Democratic Republic, DDR-6900 Jena.

The synthesis and initial characterization of the short DNA helix, d-(C1C2A3A4G5C6T7T8G9G10)<sub>2</sub>, have been reported by our laboratory (Biochemistry 19, 4688, 1980). The CH resonances of the base protons at both helical and coil states were assigned unambiguously (T<sub>m</sub> ~ 60°C at strand conc. 6mM, 0.1M NaCl, pH 7.0, phosphate buffer). The NH-N hydrogen-bonded resonances were assigned based on their relative thermal stability and the assignments were confirmed by NOE results. The <sup>1</sup>H spin-lattice relaxation measurements (T<sub>1</sub>) of all these assigned C-H base proton resonances have been determined at 300 MHz at 25°, 63°, and 80°C. The T<sub>1</sub> values at 25°C are: C<sup>1</sup>-H<sub>6</sub> - 1.61 sec., C<sup>1</sup>-H<sub>5</sub> - 1.59 sec., C<sup>2</sup>-H<sub>6</sub> - 0.90 sec., C<sup>2</sup>-H<sub>5</sub> - 1.32 sec., A<sup>3</sup>-H<sub>8</sub> - 1.20 sec., A<sup>3</sup>-H<sub>2</sub> - 1.82 sec., A<sup>4</sup>-H<sub>8</sub> - 1.21 sec., A<sup>4</sup>-H<sub>2</sub> - 2.79 sec., G<sup>5</sup>-H<sub>8</sub> - 2.04 sec., C<sup>6</sup>-H<sub>6</sub> - 1.15 sec., C<sup>6</sup>-H<sub>5</sub> - 1.43 sec., T<sup>7</sup>-H<sub>6</sub> - 0.85 sec., T<sup>8</sup>-H<sub>6</sub> - 0.99 sec., G<sup>9</sup>-H<sub>8</sub> - 1.07 sec., and G<sup>10</sup>-H<sub>8</sub> - 2.50 sec. For the coil state (80°C) the T<sub>1</sub> values of these protons increase significantly. The T<sub>1</sub> relaxation times of these assigned base protons were also measured at 500 MHz at 25° C. The data show that T<sub>1</sub> measurements are definitely frequency-dependent. The selective T<sub>1</sub> measurements of the assigned NH resonances were carried out at 360 MHz at 1°C. The T<sub>1</sub> values are: C<sup>1</sup>G<sup>10</sup> - 0.02 sec., C<sup>2</sup>G<sup>9</sup> - 0.23 sec., A<sup>3</sup>T<sup>8</sup> - 0.30 sec., A<sup>4</sup>T<sup>7</sup> - 0.33 sec. and G<sup>5</sup>C<sup>6</sup> - 0.26 sec. These studies pave the way to understanding the dynamics of the decamer helix. (Supported by NSF PCM 80-23380, NIH CA 27111 and GM 27512).

**T-PM-Po51** DNA SUPERHELICITY MEASUREMENT BY SLAB GEL ELECTROPHORESIS: IONIC STRENGTH AND DNA CONCENTRATION DEPENDENCE. Saibal K. Poddar and Jack Maniloff, Department of Microbiology, University of Rochester, Rochester, NY 14642.

Using a template similar to that described by Serwer (Anal. Biochem. 101:154, 1980), lanes of low percent agarose (0.3-0.7%) can be formed in a matrix of high percent agarose (1.5%). Since diffusion of low molecular weight components between lanes is reduced in this system, lanes can be formed with each lane containing a different concentration of ethidium bromide; thereby allowing a determination of DNA superhelix density by ethidium bromide titration-gel electrophoresis in horizontal slab gels. This system has been used to measure the superhelix density of purified viral and plasmid covalently closed circular DNA's, in the range of 2.5-8.0 Mdal and to investigate the dependence of the measured superhelicity on DNA concentration and ionic strength.

Above about 0.1 µg DNA/lane, the measured superhelicity was found to have a nonlinear dependence on the DNA concentration. Therefore, all further superhelix densities were determined using <0.1 µg DNA/lane. At low ionic concentrations (about 0.01 M), all of the DNA's studied had about the same superhelix density. This value increased between 0.01 and 0.09 M, with a different slope for each DNA. At 0.09 M, each superhelix density curve reached a characteristic saturation value, which remained constant to the highest ionic concentration (0.18 M) examined. When plotted as relative superhelicity (superhelix density at each ionic concentration divided by superhelix density at 0.18 M) vs. ionic concentration, all the DNA's fit on a single sigmoidal curve. (Supported by NIAID grant AI 07939.)

**T-PM-Po52** CIRCULAR DICHROISM STUDIES OF POLY d(G-T)·POLY d(C-A). Bruce G. Jenkins and James L. Alderfer, Roswell Park Memorial Institute, Biophysics Department, Buffalo, N. Y. 14263.

CD spectra are obtained as a function of ionic strength and temperature for an alternating purine-pyrimidine copolymer, d(G-T)·d(C-A). Spectra are determined at 25° in buffer solution (10mM Na phosphate, pH 7.0, containing 0.1mM EDTA) at various concentrations of NaCl or CaCl<sub>2</sub>. In low salt buffer, the CD spectrum of d(G-T)·d(C-A) is characterized by (1) a positive peak, 279-285nm, θ(max.)=280nm, θ(relative) = + 1.0 (2) crossover at 257nm, (3) a negative trough, 257-230nm, -θ(max) ≈ 245nm, θ(rel.) = -0.95, (4) crossover at 230nm, (5) positive band at 223nm. Addition of NaCl to the polymer (in buffer solution) results in a reduction of the positive region (279-285nm). These reductions in rotation with increasing salt are gradual and non-cooperative. Three bands can be followed, two positive at about 280 and 273nm, and a negative one at 245nm. A high salt end point in spectrum change is observed at 25° with concentrations of either 4.3M Na<sup>+</sup> or 1.8M Ca<sup>2+</sup>. At this condition, θ(relative) for the 283, 273, and 245nm bands are 0, -0.41, and -0.81, respectively. This endpoint (4.3M NaCl) is affected by temperature since at 6°, θ(rel.)-(283,273,245) are 0, -0.54, -0.81, while at 50°, 0, -0.19, -0.81, respectively. CaCl<sub>2</sub> produces similar effects. These spectral observations accord with a B- to C- type transition seen for calf thymus (CT) DNA (Biopolymers 1973, 12, 89; Biochem. 1975, 14, 1648), where salt induces a non-cooperative decrease in the positive band region (279-285nm), except no end point is reached (at 5.5M NaCl). These results are also similar to those observed for poly d(A-T) (Biopolymers, 1972, 11, 761) but different from poly d(G-C) (J. Mol. Biol. 1972, 67, 375). Although fiber data (Nature 1980, 283, 743) of d(G-T)<sub>n</sub>·d(C-A)<sub>n</sub> have been interpreted as a left-handed structure, these solution CD studies are more consistent with B- and C- type forms.



**T-PM-Po53** DNA PACKING IN THE FILAMENTOUS VIRUSES fd, Xf, Pfl, AND Pf3 AS REVEALED BY SILVER ION BINDING. A. Casadevall and L. A. Day, The Public Health Research Institute of the City of New York, New York, N.Y. 10016

Spectral changes produced by  $\text{Ag}^+$  in solutions of filamentous viruses, together with other data, show that the DNA structures in two strains, fd and Xf, are quite similar to each other but that these differ widely from unique DNA structures in two other strains, Pfl and Pf3. The principal results are large CD shifts in the near ultraviolet spectral region, which for both fd virus and Xf virus look like those produced by adding  $\text{Ag}^+$  to isolated DNAs, including superhelical DNAs. The nature of the shifts and a stoichiometries suggest that the DNA helices in fd and Xf both have bases directed toward the centers of the viruses and both have a righthanded sense. Quite different CD shifts for Pfl are consistent with a DNA structure having bases directed outward. No CD shifts at all were observed for Pf3. Similar DNA structures occur in fd and Xf in spite of different helical arrangements of the protein subunits surrounding the DNAs and different overall chemical stoichiometries. Comparisons of DNA-protein packing in all four strains are of interest in that all have gram-negative bacteria as hosts, the same overall morphology, and about the same mass-per-length.

**T-PM-Po54** AGGREGATION OF DNA BASE DERIVATIVES IN WATER. P. Martel, Atomic Energy of Canada Ltd., Chalk River Nuclear Laboratories, Chalk River, Ontario, K0J 1J0, Canada.

Solutions in heavy water of 6-methylpurine,  $\text{N}^6, \text{N}^9$ -dimethyladenine, 6-dimethylaminopurine-9-ribose (6-P-9R) and 2'-deoxycytidine have been examined by neutron diffraction. Comparison of the scattering from various molar solutions of 6-methylpurine with the scattering from its crystalline precipitates indicated base stacking in solution with a separation of  $\sim 0.34$  nm. In particular at 1.75 M the effective stacking number in 6-methylpurine solution, as seen by neutron diffraction, was found to be approximately nine. Attempts to observe similar scattering from  $\text{N}^6, \text{N}^9$ -dimethyladenine were hampered because solutions with a concentration greater than 0.02 M tended to form filamentary crystallites whose Bragg scattering increased with time. By monitoring the growth of the Bragg scattering the rate of crystalline formation was found to be describable as a second order autocatalytic reaction with a rate constant of  $2.12 \pm 0.05 \text{ M}^{-1} \text{ h}^{-1}$ . On comparing the diffraction from wet and dry crystallites it was concluded that hydrophilic interactions mediate the aggregation of both bases in water. The scattering from the nucleoside derivatives did not exhibit measurable intensity corresponding to separations of 0.34 nm. For 2'-deoxycytidine some small angle scattering was observed which indicated that very few molecules were aggregating. The scattering at small angles from 6-P-9R indicated the presence of larger clusters. Because ethidium bromide (EB) and 8-methoxypsoralen (8-MOP) are thought to be attracted to bases in DNA where they intercalate, measurements were performed to see if these mutagens might serve as centers for nucleation around which aggregation could occur. Nucleoside solutions with 0.3g/l EB and 1mg/l 8-MOP did not show any detectable change in diffraction pattern as compared with pure solutions.

**T-PM-Po55** LASER LIGHT SCATTERING AND ABSORBANCE HYPERCHROMICITY ANALYSES OF *E. COLI* 4.5S RNA.

D. Bourgaize, C. Farrell, L. Hsu<sup>+</sup>, K. H. Langley\* and M. J. Fournier. Departments of Biochemistry and Physics (\*), University of Massachusetts, Amherst, MA 01003 and Department of Chemistry (+) Mount Holyoke College, South Hadley, MA 01075.

Quasi-elastic laser light scattering (LLS) and absorbance at 260 nm have been used to study the effect of solution conditions on the structure and thermal unfolding of the metabolically stable *E. coli* 4.5S RNA. LLS measurements of the translational diffusion coefficient and hyperchromicity measurements were made for  $[\text{Mg}^{+2}]$  of 0 to 10 mM, and ionic strengths of 0.1 to 0.35 M. The molecule exhibits an unusually high degree of stability as evidenced by the high temperatures needed to achieve thermal denaturation in both experimental techniques. Optical  $T_m$ 's range from 79°-86°C with transitions  $\sim 25^\circ\text{C}$  wide. Broad transitions and shoulders at temperatures higher and lower than the  $T_m$  peak in differential plots suggest that there are regions of differing stabilities. The optical  $T_m$  shows little dependence on ionic strength, but increases in  $[\text{Mg}]$  at constant ionic strength increases the stability of the molecule. In the LLS experiments, the diffusion coefficient does not begin to decrease until  $T > 70^\circ\text{C}$ . Neither the diffusive melting nor diffusion coefficient at infinite dilution ( $D_0$ ) at  $20^\circ\text{C}$  show dependencies on  $[\text{Mg}^{+2}]$  or ionic strength. The  $D_0$  values do allow a calculation of a hydrodynamic model, that of a prolate ellipsoid of axial ratio  $20 \pm 7$ . These results are consistent with the most stable hypothetical secondary structures that can be formed in which  $\sim 80$  of 114 bases are paired to form a near-perfect hairpin helix. (Supported by NSF Grant PCM 8021136 to KLH and NIH Grant GM 19351 to MJF).

**T-PM-Po56** SYNTHESIS AND CHARACTERIZATIONS OF MODIFIED DECADEOXYNUCLEOTIDES. L.-S. Kan, D.M. Cheng, E.E. Leutzinger, and P.S. Miller, Division of Biophysics, The Johns Hopkins University, Baltimore, Maryland 21205.

The objective of this study is to observe the conformational properties of a series of specifically alkylated decadeoxyribonucleotides (helices) with the base sequence:



The helices carry modifications including an alkylated phosphate group, alkylated bases, and an apurinic site in the central region. At present the following oligonucleotides have been synthesized: d-Gp(Et)A's (isomers 1 and 2), d-CCAAGA, d-CCAAGp(Et)A's, d-TCTTGG, d-CCAAGATTGG, d-CCAATCTTGG, and d-CCAAGp(Et)ATTGG's. These oligomers were characterized by uv spectroscopy, by enzymatic digestion with snake venom phosphodiesterase, and by  $^1\text{H}$  and  $^{31}\text{P}$  NMR spectroscopy. The strategy is to understand the perturbational effect of helix modification in a stepwise manner. For example, studies on d-GpA and the two d-Gp(Et)A isomers showed that the base stacking of G and A are left-handed and the extent of the stacking of isomer 2 is close to that of d-GpA while both are more extensively stacked than isomer 1. Studies on d-CCAAGA and d-CCAAGp(Et)A show that the backbone conformations of d-CCAAG moieties in these hexamers are the same. Finally, NMR studies on the self-association of d-CCAAGATTGG, d-CCAATCTTGG, and d-CCAAGp(Et)ATTGG indicate the following stabilities:  $(\text{CCAAGATTGG})_2 > (\text{CCAAGp(Et)ATTGG isomer 2})_2 > \text{isomer 1} > (\text{CCAATCTTGG})_2$ . No hydrogen-bonds between G and A were observed. However, the melting of these helices in aqueous solution is still from the ends towards the middle, in spite of the presence of non-bonded bases in the middle. (Supported by NCI CA 27111).

**T-PM-Po57** COUNTERION CONDENSATION IN POLYELECTROLYTES: G.V. Ramanathan and C.P. Woodbury, Jr., Department of Mathematics, University of Illinois at Chicago Circle, and Department of Medicinal Chemistry, University of Illinois Medical Center, Chicago, Illinois, 60680.

Modelling the polyion as a line charge (length  $2L$ ) in a dilute solution of small ions, with distance of closest approach  $\alpha$ , we have studied the BBGKY hierarchy of equations under the conditions  $\alpha \ll L \ll \kappa^{-1}$  ( $\kappa^{-1}$  is the Debye length). In the bulk limit the hierarchy for polyion-small ion correlations decouples from the small ion-small ion hierarchy. From estimates we show the Born-Green-Yvon (BGY) approximation will suffice to describe counterion "condensation". We solve the BGY asymptotically as  $\kappa\alpha \rightarrow 0$ . For subcritical polyion charge densities we obtain a solution corresponding to the Debye-Huckel approximation. For charge densities above critical we find that for large separations the polyion-counterion correlations behave as if the polyion charge density were at the critical value, i.e. as if counterions had "condensed" to lower the charge density to precisely the critical value. This is due to the counterion correlation at short range, the strong effect of which is taken into account in the BGY approximation. We find the precise order of  $L$  for the onset of "condensation" in terms of  $\kappa$ ,  $\alpha$ , and the charge density.

**T-PM-Po58** FLUORESCENCE ENERGY TRANSFER AND NMR STUDIES WITH Co-Zn RNA POLYMERASE. Dipankar Chatterji and Felicia Y.-H. Wu, Department of Pharmacological Sciences, State University of New York at Stony Brook, New York 11794.

*E. coli* RNA polymerase (RPase) contains two intrinsic Zn ions, one in the  $\beta$  subunit and the other in the  $\beta'$  subunit. We have substituted *in vitro* the Zn ion located in the  $\beta$  subunit with Co to give the Co-Zn hybrid enzyme. Co-Zn RPase is as active as Zn-Zn enzyme and exhibits an intense charge transfer band at 400 nm ( $\epsilon=3000$ ). When Co-Zn core RPase ( $1 \times 10^{-7}\text{M}$ ) was added to the equimolar isolated  $\sigma$  subunit in which a specific cysteine residue was covalently labeled with N-pyrene maleimide (PM- $\sigma$ ), 50 and 39% quenching of the PM- $\sigma$  fluorescence were observed, respectively, in the absence and presence of a short DNA template, oligo[d(A-T)](60 $\pm$ 2 b.p.). In contrast, the corresponding fluorescence quenching caused by Zn-Zn core RPase was 17 and 14%, respectively, under similar conditions. The difference in the extent of fluorescence quenching was due to excited-state energy transfer from the PM chromophore to the Co ion in the enzyme. From the measured energy transfer efficiencies, the distances between the intrinsic metal ion in the  $\beta$  subunit and the specific cysteine residue in the  $\sigma$  subunit were calculated to be 22 and 33 Å, respectively, with or without DNA template. These distances were not significantly altered by addition of substrate ATP. The interaction between Co-Zn RPase and ATP in the presence of DNA template was studied by NMR spectroscopy. Titrations of the paramagnetic relaxation rate of bound water on Co-Zn RPase with ATP indicated that ATP bound tighter to the enzyme in the presence of template ( $K_d=0.0088\text{ mM}$ ) than in the absence of template ( $K_d=0.15\text{ mM}$ ). The implication of these results to the role of the intrinsic metal in RPase will be discussed. (Supported by NIH and NSF grants).

**T-PM-Po59** *IN SITU* REPAIR IN LESS ACCESSIBLE REGIONS OF MAMMALIAN DNA. J.V. Wierowski and K.T. Wheeler (Intr. by T.D. Griffiths), Cancer Center, University of Rochester, Rochester, NY, 14642

Recently we demonstrated that *in situ* repair, as measured on alkaline sucrose gradients in zonal rotors, of radiation-induced DNA damage in intracerebral 9L tumor cells and cerebellar neurons follows biphasic kinetics. The data suggested that the fast and slow phase most likely represented repair in very accessible and less accessible regions of the genome, respectively. The half-times ( $T_{1/2}$ ) of the slow phase in both tumor cells and neurons increased as a function of dose indicating that this repair process was saturable. In the study reported here, Fisher 344 rats bearing intracerebral 9L tumors were whole brain irradiated with two 1250 or two 2500 rad doses of Cs-137  $\gamma$ -rays separated by 15 min to 24 hr and the repair kinetics after the second dose was measured. In general, the  $T_{1/2}$  of the slow phase in both tumor cells and neurons was faster than that expected on the basis of the amount of damage present in the less accessible regions, but slower than that found after a single 1250 or 2500 rad dose. The  $T_{1/2}$  of the slow phase remained constant if doses were separated by 15 min to 2 hr. When repair of the first dose was complete (24 hr), the  $T_{1/2}$  of the slow phase after the second dose returned to the single dose  $T_{1/2}$ . A model for repair of radiation-induced DNA damage in less accessible regions of the mammalian cell genome will be presented to explain these single and split-dose repair kinetics. (Supported by grants CA-21662, CA-11198 and CA-09363).

**T-PM-Po60** RATE OF DNA REPAIR IN SUNLIGHT-IRRADIATED HUMAN CELLS. G. J. Kantor and C. Ritter. Biological Sciences Department, Wright State University, Dayton, Ohio 45435.

Sunlight induces pyrimidine dimers in DNA of exposed human cells (Trosko, et al., *Nature* 228: 358, 1970). The rate of excision of these pyrimidine dimers was determined using cultured populations of a normal excision-repair proficient human diploid fibroblast strain (WS-1) and a repair deficient xeroderma pigmentosum fibroblast strain (XP12BE, group A). Cells covered with 2 mm of HEPES-buffered saline were exposed to unfiltered sunlight. Temperature of the buffer was maintained at 22-25°C during exposures. Exposures were done between 11:00 AM and 1:00 PM Eastern Standard Time during the period of May 4 - July 23, 1981 in Dayton. Irradiated cells were maintained in a nondividing state using a normal culture medium supplemented with 0.5% fetal calf serum. Pyrimidine dimers were quantified in DNA extracted at various times after sunlight exposure using a dimer-specific endonuclease from *Micrococcus luteus*. The number of nicks, and thus pyrimidine dimers, in endonuclease-treated DNA was determined using alkaline sucrose gradients. The sunlight exposures used (5 and 20 min.) induced a number of dimers equivalent to a UV (254 nm) exposure of 1 and 4 J/m<sup>2</sup>. We found that, for both the normal and XP strain, the excision rates of sunlight-induced pyrimidine dimers were the same as that observed for the excision of UV-induced pyrimidine dimers (Kantor and Setlow, *Cancer Res.* 41: 819, 1981). No sunlight induced inhibition or stimulation of DNA repair was observed in either strain. (Research supported by NIH grant CA16477).

**T-PM-Po61** VISCOELASTIC RECOIL, THE MEASUREMENT OF DNA STRAND BREAKS, AND A METHOD FOR DISTINGUISHING BETWEEN REPAIR AND DEGRADATION OF STRAND-BREAK-INDUCED DNA CONFORMATION CHANGES.

Christopher S. Lange, Dept. of Radiation Oncology, SUNY Downstate Med. Ctr., Brooklyn, NY 11203.

The viscoelastic relaxation behavior of shear-stressed DNA can determine the size (from  $\tau_{11}$ ) and number concentration (from  $\Gamma_{11}$ ) of the largest such molecules present. This holds for an initially monodisperse population of intact random coil molecules (e.g., viral genomes). We have shown that this method can be calibrated against known numbers of viral genomes to yield a  $\Gamma_{11} r_0$  vs.  $c$  (DNA concentration) regression line and that  $\Gamma_{11} r_0$  can therefore yield the number of surviving INTACT DNA molecules (6th ICRR, C28-2, 1979; *Biophys. J.*, 33:269a, 1981), since broken molecules cease to contribute to  $\Gamma_{11} r_0$ . Thus, intact DNA survival curves were derived for T4c DNA. Circular relaxed genomes (e.g., *E. coli*) can also be handled in this way. In superhelical nucleoids, the induction of the FIRST break relaxes a domain (loop) which increases the effective contour length of the DNA and introduces a new  $\tau_{11}$  and  $\Gamma_{11}$  for the new longest molecules. Thus, for condensed DNA, damage can be expressed as an increase in  $\tau_{11}$ . Return of the  $\tau_{11}$  value to that of the original population can come about in either of two very different ways. REPAIR or DEGRADATION of the extended loop. Degradation must not be confused with repair. If the nucleoid minus the loop has a net contour length < that of the intact nucleoid,  $\Gamma_{11} r_0$  for the intact nucleoids will be < the preirradiation value and the difference will yield the number of molecules degraded. If the effective contour length is indistinguishable from the original, in spite of the loss of a domain, then repair and degradation will not be distinguishable by viscoelastometry alone. Supported by DOE Contract No. DE-AC02-80EV-0503.

**T-PM-Po62** MOLECULAR MECHANISM OF IN VITRO 50S RIBOSOME ASSEMBLY. KIN-PING WONG, LUC SINH NGUYEN, & KURT F. KESSLER. DEPT. BIOCHEMISTRY, UNIVER. KANSAS-MEDICAL CENTER, K.C., KS. 66103.

The molecular mechanism of the in vitro assembly of E. Coli 50S ribosomal subunit has been studied by sedimentation velocity [Nguyen, L.S. & Wong, K.P. (1981) *Fed. Proc.* 40, 1898] and sedimentation equilibrium as well as circular dichroism (CD). The different molecular species occur during the various steps of the reconstitution were also characterized.

Sedimentation equilibrium analyses indicated that the 23S RNA exists as a homogeneous monomer ( $1.03 \times 10^6$ ) in TM-4 and as a heterogeneous monomer ( $1.08 \times 10^6$ ) and dimer ( $1.70 \times 10^6$ ) system in TM-20 + RM. The presence of the dimer of 23S RNA suggests the existence of a RNA-protein dimer in the same buffer during the reconstitution. Results from difference CD show various changes during each of the steps of the assembly to form the 50S subunit. In addition, the first heat incubation (44°C) appears to be reversible, while the second heating step (50°C) appears to be irreversible. A possible model on the conformation and shape changes of the various molecular species during the course of the assembly is proposed. The binding of approximately 2/3 of the total proteins from the 50S subunit (TP50) helps the folding of the RNA into a more compact RI(1) particle. The heating at 44°C "opens up" the RI(1) into a more extended RI\*(1) particle, presumably exposing the binding sites for the remaining proteins. Addition of 20 mM  $Mg^{2+}$  allows the RNA to assume a more compact shape and stabilizes the RI(2) particle which enables the formation of the 50S subunit. The last step involves the heating of the RI(2) particle to form the 50S subunit consists of a conformation change resulting from unfolding of some of the RNA secondary structure to form the stable 50S subunit. This last step is irreversible. (Supported by NIH grants GM22962, HL18905 and GM70628)

**T-PM-Po63** UNDERSTANDING THE MOTIONS OF NUCLEIC ACIDS: ANGULAR INTERDEPENDENCE AND CONFORMATION TRANSITIONS. A.R. Srinivasan and W.K. Olson, Chemistry Department, Rutgers University, New Brunswick, New Jersey 08903.

A simple theoretical procedure is introduced to identify and measure the interdependency of torsional variables in the polynucleotide chain backbone. Most strongly correlated rotational motions are associated with bonds in parallel alignment - such as second-neighbor rotations separated by a trans linkage or third neighbor angles connected by an intervening gauche, gauche torsional sequence. Provided the parameters vary in the opposite rotational sense, it is possible for second-, third-, and higher-neighbor torsions to rotate "freely" over their entire angular ranges without destroying the parallel stack of the polynucleotide helix. On basis of this approach relative flexibilities of DNA and RNA may be compared. The information is also used to examine the detailed conformational pathway for the smooth transition of right-handed B-DNA to the unusual left-handed Z-form. (Supported by USPHS Grant GM-20861).

**T-PM-Po64** THE DISSOCIATION MECHANISM OF COOPERATIVELY BOUND T4 GENE 32 PROTEIN-NUCLEIC ACID COMPLEXES. Timothy M. Lohman, Department of Biochemistry and Biophysics, Texas A&M University, College Station, Texas 77843.

The dissociation of cooperatively bound T4 gene 32 protein from single stranded homopoly-nucleotides has been investigated using stopped-flow techniques which monitor the increase in the intrinsic tryptophan fluorescence of the protein upon dissociation. Both [NaCl] jumps and competition studies with a higher affinity polynucleotide were used to measure the apparent dissociation rate constant for the irreversible dissociation, under a variety of solution conditions. The data quantitatively support a model in which the dominant (and only observable) mode of dissociation is that of singly contiguous molecules from the ends of protein clusters. The salt dependence of this process suggests that singly contiguous gene 32 protein dissociates directly from cluster ends at high salt, but at low salt the dominant pathway is dissociation of singly contiguous protein via a bound isolated intermediate. That is to say, the protein seems to "slide" off the end of a cooperatively bound protein cluster to form an isolated gene 32 protein which then dissociates rapidly from the nucleic acid. Through application of Berg and Blomberg's analysis of one-dimensional diffusion of proteins we estimate that T4 gene 32 protein can translocate along single stranded DNA with an apparent one-dimensional diffusion coefficient of  $\Gamma \sim 10^{-9} \text{ cm}^2 \text{ sec}^{-1}$ . This does not necessarily mean that entire clusters of T4 gene 32 protein can translocate, however, translocation of even isolated protein molecules will facilitate the formation of cooperative interactions by enabling the protein to sample many DNA binding sites until a cooperative interaction is formed.

**T-PM-Po65** INTERNAL MOBILITY OF RNA IN TWO PLANT VIRUSES BY  $^{31}\text{P}$  NMR. R. Virudachalam, Douglas C. McCain, John L. Markley, Sherin S. Abdel-Meguid, Michael G. Rossmann, and Patrick Argos, Departments of Chemistry and Biological Sciences, Purdue University, W. Lafayette, IN 47907

The motional state of RNA in southern bean mosaic virus (SBMV) and belladonna mottle virus (BDMV), have been analyzed by  $^{31}\text{P}$  NMR. Both these viruses are RNA containing spherical particles with a diameter of about 288 Å. The RNA content in SBMV is about 22 percent by weight whereas that of BDMV is about 37 percent. The capsids in both the cases are made up of 180 identical protein subunits. The coat protein of SBMV contains an N-terminal arm with a large number of basic residues which is believed to interact with the RNA to stabilize the virus structure. BDMV lacks such a basic arm, and the virus structure is stabilized mainly by capsid protein-protein interactions.  $^{31}\text{P}$  spin-lattice relaxation and line width measurements over a wide range of pH show that the motional state of RNA is unchanged in native SBMV whereas in the case of native BDMV or EDTA treated SBMV (swollen) the RNA undergoes a phase transition around neutral pH. The data can be analyzed to show the time scale of these motions. The mechanism for spin-lattice relaxation and nuclear Overhauser enhancement will be discussed. The  $^{31}\text{P}$  NMR linewidth of BDMV is much smaller than for native SBMV, suggesting higher mobility for the RNA in the former. Very low concentrations of paramagnetic ions broaden considerably the  $^{31}\text{P}$  signal from BDMV suggesting that the capsid structure is permeable to metal ions.

(Supported by NIH grants GM 19907, AI 11219, and RR 01077 and NSF grant AI 11219.)

**T-PM-Po66** AN ANALYSIS OF THE INFLUENCE OF THE SPATIAL DISTRIBUTION OF THE SITES ON THE KINETICS OF PROTEIN-NUCLEIC ACID REACTIONS, Sharlyn J. Mazur, M. Thomas Record, Jr. (Intr. by Douglas C. Kramp), Department of Chemistry, University of Wisconsin, Madison, Wisconsin 53706.

The rates of diffusion limited reactions are determined, in part, by the size and shape of the reactants. In the reaction of a protein with a nucleic acid, the configuration of the nucleic acid or the position of a specific sequence in the molecule may influence the observed kinetics. We have developed a theoretical description of protein-nucleic acid reactions with particular attention to the distribution of sites on the nucleic acid. Analytic and numerical methods have been combined to obtain the solution of the reaction-diffusion equation. The reactive and diffusive terms are coupled, leading to the presence of more than one time constant and a mixing of local and global processes. In the limit of low concentrations of nucleic acid molecules, the transition from a reaction-limited rate to a diffusion limited rate is interpreted as a transition from a site-based reaction to a molecule-based reaction. With the assumption of an initial equilibrium with nonspecific sites, the theory is extended to describe the reaction of a protein with a specific sequence of the nucleic acid. The effect of the position of the specific sequence in the nucleic acid and of other geometric features is investigated. The results are compared with those of other theories and with published data from the *lac* repressor-operator system.

**T-PM-Po67** MECHANISM OF INITIATION FACTOR 3 AND RIBOSOMAL PROTEIN S1 BINDING TO RIBOSOMES.

D.J. Goss, L.J. Parkhurst, and A.J. Wahba, Dept. of Chemistry, University of Nebraska, Lincoln, NE 68588, and Dept. of Biochemistry, Medical School, University of Mississippi, Jackson, MS 39216.

The interactions of initiation factor 3 (IF3) and ribosomal protein S1 as a function of Mg ion concentration have been studied by light-scattering and fluorescence polarization stopped-flow measurements. The association reaction of 30S and 50S subunits from *E. coli* ribosomes and the dissociation of 70S ribosomes have been followed by light-scattering as a function of Mg ion concentration. The binding of fluorescently-labelled IF3 to 30S and to 70S ribosomes has been followed by fluorescence polarization studies. The model for treating these processes consists of 4 reactions, three of which are thermodynamically independent. The association reaction of 30S + 50S subunits shows approximately 7th order Mg ion dependence below 5 mM Magnesium. Two forms of IF3 were found that differed markedly in their rates of binding to 30S subunits. Type I IF3 binds to 30S subunits one thousand times more slowly than does type II, but the equilibrium constants are essentially the same for both types. The simplest model that explains both the light-scattering and anisotropy data for both types of IF3 is one that includes as a necessary step the association of 30S-IF3 with 50S subunits to form a 70S-IF3 complex. This step is not allowed in the anti-association model. Ribosomal protein S1 has been labelled with 1,5 IAEDANS, a fluorescent SH reagent. Binding of labelled S1 to S1-deficient ribosomes has been followed by monitoring changes in fluorescence polarization. The affinity of 70S ribosomes for S1 is approximately 30 times greater at 10 mM Magnesium than at 5 mM. Grant Support: NIH HL 15, 284-09, GM 25451, and NSF PCM 8003655.

**T-PM-Po68** CRYSTALLIZATION OF RESOLVASE, A DNA-BINDING ENZYME INVOLVED IN TRANSPOSITION

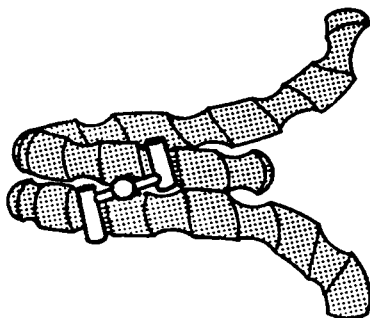
Patricia C. Weber and T. A. Steitz, Department of Molecular Biophysics and Biochemistry, Yale University, New Haven, Connecticut 06511 U.S.A.

Transposable elements or transposons are specific sequences of DNA which can move from site to site in the chromosome. The 5700 base pair  $\gamma\delta$  element codes for two-proteins required for its transposition (Reed, R. R., *Proc. Natl. Acad. U.S.A.* (1981) 78, 3428-3432). The first protein, transposase, is involved in element insertion and replication. Subsequent excision of the transposon requires resolvase, the second protein coded for by the transposon. Resolvase also acts as a repressor to prevent expression of the entire  $\gamma\delta$  element.

The resolution reaction in vitro requires an appropriate supercoiled DNA substrate, resolvase and  $Mg^{+2}$  (Reed, R. R. *Cell* 25 (1981) 713-719). In the absence of  $Mg^{+2}$ , the reaction terminates with an intermediate DNA-protein complex. We have crystallized resolvase under magnesium-free conditions. Preliminary characterization of these crystals indicates diffraction to at least 3 Å resolution and suggests that the 42,000 m w dimer occupies the crystallographic asymmetric unit.

**T-PM-Po69** TRIPLET ANISOTROPY DECAY STUDIES OF NUCLEOSOMES - M. Hogan, J. Wang, R. Austin, C. Monitto and J. Karohl (Princeton University)

We have extended our studies of the brownian motion of DNA fragments to purified nucleosome core particles. The 146 base-pair DNA fragment bound to the nucleosome core particle is not completely rigidly constrained on the surface of the nucleosome core particle but instead has a limited degree of torsional freedom. The temperature and viscosity dependence of the anisotropy decay for two different triplet probes will be compared with theoretical predictions in order to quantify the effect that the histone proteins have upon the DNA rigidity.

**T-PM-Po70** A MODEL FOR CATABOLITE ACTIVATOR PROTEIN BINDING TO SUPERCOILED DNA. F. R. Salemme, Department of Molecular Biophysics and Biochemistry, Yale University, New Haven, Connecticut 06511

Recent x-ray structural studies of catabolite activator protein (CAP) have suggested that it binds to a left-handed form of B-DNA (McKay and Steitz [1981] *Nature*, 5809, 744-9). This model was based on examination of the orientation of a pair of diad-related  $\alpha$ -helices in the dimeric CAP molecule which can only make major groove interactions if the DNA is left-handed. However, an alternative model based upon observed structural properties of non-specifically bound CAP-DNA complexes (Chang, et al., [1981] *J. Mol. Biol.* 150, 435-9) suggests that CAP may bind to right-handed supercoiled DNA, as shown in the Figure. The consequences and potential significance of this alternative mode of CAP-DNA interaction to the molecule's control and activator functions will be described.

**T-PM-Po71** MOLECULAR MECHANISM OF CONTROL OF TRANSCRIPTION AT THE *E. coli* GALACTOSE OPERON. Stephanie H. Shanblatt and Arnold Revzin, Department of Biochemistry, Michigan State University, East Lansing, MI 48824.

The interactions of RNA polymerase and of the catabolite activator protein (CAP) with cloned DNA fragments containing the galactose operon control region have been investigated using a number of physical methods. This operon displays both a CAP-sensitive and a CAP-insensitive mode of transcription. A gel electrophoresis technique revealed the presence of long lived polymerase-promoter and CAP-promoter complexes at ionic conditions where binding of the proteins to non-specific DNA regions is negligible. This approach was used to measure thermodynamic and kinetic parameters for the DNA binding of the two regulatory proteins. In addition, CAP-polymerase-promoter interactions have been studied (with and without cyclic AMP) by centrifugation methods. Transcription assays have been used to monitor both the number of RNA transcripts and the degree of initiation occurring from CAP-sensitive and CAP-insensitive start sites under various solution conditions. These studies are aimed at elucidating questions such as which protein binds first to the promoter, does polymerase in a tight complex with the CAP-insensitive promoter move to the CAP-sensitive site if CAP-cAMP is added, if such movement occurs must the enzyme dissociate from the DNA in the process, etc.

**T-PM-Po72** MOLECULAR STRUCTURE OF TOBACCO MOSAIC VIRUS BY FIBER DIFFRACTION. Gerald Stubbs, Rosenstiel Center, Brandeis University, Waltham, MA 02254 and Lee Makowski, Department of Biochemistry, College of Physicians and Surgeons of Columbia University, New York, NY 10032.

Tobacco mosaic virus (TMV) is a helical virus, 3000Å long and 180Å in diameter. The repeating unit is 49 subunits in 3 turns of the helix. Each subunit has a MW of 18,000 and binds 3 nucleotides of RNA. The structure of TMV was determined at 4Å resolution by Stubbs, Warren & Holmes (Nature 267, 216-221 (1977)) using fiber diffraction from oriented gels. This required 6 heavy-atom derivatives. The large number of derivatives is required because the particles in the gel, although aligned approximately parallel to an axis, take up random orientations about that axis. Thus the diffraction pattern is cylindrically averaged, and information is lost. This information can be regained with the extra heavy-atom derivatives. Another source of information is the fine splitting of the layer lines in the diffraction pattern. We have shown that this splitting can be measured, and even the difference in splitting from one heavy-atom derivative to another can be measured in favorable cases. We have combined this information with the isomorphous replacement information, and this has enabled us to calculate maps with fewer heavy-atom derivatives, and to extend the resolution possible given the available number of derivatives. (This work was supported by NIH grants GM25236 to G.S. and CA29522 to L.M.)

**T-PM-Po73** MODELS OF FORWARD INHIBITION CHARACTERISTICS IN PHAGE. John Aldridge, Dept. Genetics, Children's Hospital, Boston, Mass. 02115.

Forward inhibition of flow may generate a single peaked flux vs. force characteristic as in a voltage stable tunnel diode. The same characteristic may be generated by combined back inhibition (negative feedback) and back activation. Bistability and periodicity are expected in networks with these elements. The mutual coupling of two such elements might also cause random dynamical behavior (chaos). Bifurcation between qualitative behaviors may depend on parameters affecting the shape of the single peak characteristic. An assay of shape change induced by parameter alteration might be possible through monitoring dynamical response. Because forward inhibition characteristics have been described in bacteriophage operator - repressor interaction, and because the association constants of repressor at binding loci are subject to experimental manipulation through site directed mutagenesis, the construction of DNA regulatory networks capable of being "tuned" to elicit different qualitative dynamics may be possible. Example networks and technical difficulties involved in such "genetic engineering" will be discussed.

**T-PM-Po74** IDENTIFICATION OF POLYPEPTIDES RELATED TO CAP BINDING PROTEINS(CBP) IN CYTOPLASMIC RNP PARTICLES OF CHICK EMBRYONIC MUSCLE. A.K.Mukherjee<sup>1</sup>, D.Chakraborty<sup>1</sup>, S.Sarkar<sup>1</sup>, K.A.W. Lee<sup>2</sup> & N.Sonenberg<sup>2</sup>. <sup>1</sup>Dept. Muscle Res., Boston Biomed. Res. Inst., Boston, MA 02114 & <sup>2</sup>Dept. Biochemistry, McGill Univ., Quebec, Canada.

Using monoclonal antibody to CBP of rabbit reticulocytes we have studied the localization of proteins which react with anti-CBP in cytoplasmic RNP particles of chick embryonic muscle. Four types of particles were used: the nonpolysomal 20-40 S mRNP(CmRNP), polysomal mRNP(PmRNP), the poly(A)-protein fragments of PmRNP, and the cytoplasmic 10 S RNP(iRNP) containing a 4 S translation inhibitory RNA (JBC. 256, 5077, 1981). The cross-reacting antigens were detected by indirect immunostaining of nitrocellulose blots of SDS-PAGE of the particles using horse raddish peroxidase coupled antibody. Among the multiple Coomassie-blue stained protein bands (Mr 12,000 - 100,000) present in 10 S iRNP and CmRNP, only one band (80K) reacted with anti-CBP. When immunostaining was carried out in gel blots of the isolated proteins instead of the particles, two new cross-reacting bands (50K and 24K) appeared and the 80K cross-reacting band was either absent or decreased concomitantly. The 80K cross-reacting band was absent in crude or purified PmRNP and their poly(A)-protein segments, although a Coomassie blue stained band (78K) of the poly(A)-associated protein was present. It is concluded that (i) the 80K cross-reacting band is specifically present in 10 S iRNP and CmRNP but is absent in PmRNP; (ii) this 80K protein is distinct from the 78K poly(A)-associated protein of mRNP particles; and (iii) the 80K cross-reacting protein may be a precursor of the 50K and 24K cross-reacting bands suggesting that the polypeptides related to CBP may undergo specific processing.

**T-PM-Po75** TRANSLATIONAL CONTROL AND OTHER LOW MOLECULAR WEIGHT RNAs ISOLATED FROM MUSCLE mRNPs. B. Mroczkowski\*, T. L. McCarthy\*, E. Siegel\*, S. M. Heywood, Genetics and Cell Biology Section, University of Connecticut, Storrs, Connecticut 06268.

mRNP particles exhibiting a sedimentation range between 10-40S have been purified from chick embryonic skeletal muscle by the use of sucrose density gradient and metrizamide buoyant density centrifugation. Three predominant low molecular weight RNAs are routinely isolated from these particles; one of which (102 nucleotides) has a homologous sequence to tRNA isolated from myosin heavy chain mRNPs (110-80S). The 10-40S mRNP-tRNA interacts specifically with mRNP associated mRNAs encoding for contractile proteins; this includes myosin heavy chain mRNA. This interaction has been characterized using *in vitro* translation inhibition, as well as complex formation involving mRNA-tRNA solution hybridization. We have also determined that the poly tail associated with these mRNAs is capable of hybridizing with tRNA, therefore indicating a partial mechanism by which the observed interaction occurs. However, this does not account for the specificity of the interactions (no translation inhibition or complex formation was observed when viral RNA or mRNAs isolated from heterologous cell systems were used). It appears that other sequences within the contractile protein mRNAs are required to endow such specificity. The sequences of the 88 and 150 nucleotides low molecular weight RNAs present in the 40S mRNP particles have been determined. The function of these RNAs is under study. (Supported by NIH Grant #HD03316 and a MDA post-doctoral fellowship)

**T-PM-Po76** THE EFFECT OF LIGANDS ON THE AGGREGATION AND CONFORMATION OF *E. COLI* RNA POLYMERASE; S. L. Shaner, R. R. Burgess, and M. T. Record, Jr., Chemistry Department, University of Wisconsin, Madison, WI 53706.

The aggregation equilibria of *E. coli* RNA polymerase are affected significantly by the identity of the anion, but are apparently insensitive to the identity of the cation. Using sedimentation velocity, we have compared the salt dependence of the transition from monomer to tetramer of core polymerase in NaCl, NH<sub>4</sub>Cl, NaI, and NaF. The transitions in NaCl and NH<sub>4</sub>Cl were identical. Variation of the anion shifts the concentration range over which the transition occurs. We observe the following ordering for concentrations at the midpoint of this transition: [NaI] < [NaCl] < [NaF]. We also find that the number of anions released per monomer incorporated into the aggregate is independent of anion type. In addition, we are examining allosteric effects on the conformation of the protomeric forms of core and holo RNA polymerase using difference sedimentation velocity to determine directly the change in sedimentation coefficient of RNA polymerase upon binding of a ligand. This difference can be decomposed into that resulting from the change in buoyant mass and that resulting from a change in frictional coefficient (i.e., in conformation). We are investigating potential allosteric effectors which are known to affect *in vitro* transcription or are implicated in control of *in vivo* RNA synthesis.



**T-PM-Po77** VARIABILITY OF COAT PROTEIN STRUCTURES AND INTERACTIONS OF FILAMENTOUS BACTERIAL VIRUSES. B. Prescott and G.J. Thomas, Jr., Dept. of Chem., Southeastern Massachusetts University, N. Dartmouth, MA 02747 and P.D. Boyle and L.A. Day, Dept. of Biochem., The Public Health Research Institute, New York, NY 10016.

Laser Raman spectra have been obtained as a function of temperature in the range 0 to 80°C, and as a function of salt concentration in the range  $0.001 < [\text{Na}^+] < 0.15\text{M}$ , for the following filamentous bacterial viruses: fd, Ike, Ifl, Pfl, Xf and Pf3. The Raman data reveal remarkable variability of structure in each virus, particularly with respect to changes in temperature. The temperature profile of a given virus, as revealed by its Raman line frequencies and intensities, is usually different in solutions containing low salt ( $0.001\text{M Na}^+$ ), than in solutions containing moderate ( $0.05\text{M Na}^+$ ) or high salt ( $0.15\text{M Na}^+$ ) concentration. Although the coat protein chains of all six filamentous bacteriophages are highly  $\alpha$ -helical at physiological conditions, the precise extent of  $\alpha$ -helicity and its vulnerability to change with adjustments in temperature and salt concentration are significantly different in each virus. Refinement of the laser Raman spectra by computer averaging techniques and by use of spectral subtraction routines allow identification of specific amino acid residues involved in the structure transitions observed here for fd, Pfl, Ike and Ifl, and previously for Pf3 and Xf (Thomas and Day, Proc. Nat. Acad. Sci. U.S.A. (1981) 78, 2962-2966; Thomas et al., Prog. Clin. Biol. Res. (1981) 64, 429-440). A new conformation sensitive protein mode has also been identified in the Raman spectrum of each virus, and its assignment is suggested by analogy with spectra of model compounds.

Supported by N.I.H. Grants AI 09049, AI 11855 and AI 18758.

**T-PM-Po78** HYDRODYNAMIC DETERMINATION OF THE MOLECULAR WEIGHT, DIMENSIONS, AND STRUCTURAL PARAMETERS OF PF3 VIRUS. J. Newman, L.A. Day, and D. Eden, Department of Physics, Union College, Schenectady, New York 12308, The Public Health Research Institute, New York, New York 10016, and Department of Chemistry, Yale University, New Haven, Connecticut 06520.

Measurements of the translational,  $D_T$ , and rotational,  $D_R$ , diffusion coefficients of Pf3 virus by low-angle polarized intensity fluctuation spectroscopy and field-free transient electric birefringence, respectively, give a length of  $720 \pm 25$  nm and diameter of  $6.5 \pm 1.5$  nm upon simultaneous solution of the Broersma equations for rigid rods. Sedimentation coefficient and density increment values obtained under identical solvent conditions as those of  $D_T$  give a molecular weight of  $(13.2 \pm 0.8) \times 10^6 \text{ g mol}^{-1}$ . Combining these results with the molecular weight of Pf3 DNA yields a number of protein subunits of  $2590 \pm 175$  and a non-integral ratio of nucleotides to protein subunits of  $2.30 \pm 0.17$ . This ratio as well as the mass-per-length,  $18300 \pm 1300 \text{ g mol}^{-1} \text{ nm}^{-1}$ , are in good agreement with corresponding values for fd virus despite significantly different values for both the nucleotide and protein subunit axial repeat distances.

**T-PM-Po79** THE PITCH CONNECTION AND OTHER GEOMETRICAL RELATIONS, APPLICABLE TO DNA-PROTEIN PACKING IN FILAMENTOUS BACTERIAL VIRUSES. C. J. Marzec and L. A. Day, The Public Health Research Institute of the City of New York, New York, N.Y. 10016.

The structural similarities and differences among the filamentous viruses are considered, with a view toward explaining the similarities as expressions of elementary geometrical constraints and the differences as allowed variations of these expressions. Similarities are such items as virion mass/length, diameter, rotation angles, and diffraction patterns; differences appear in integral and non-integral stoichiometries, subunit axial translations, and number and composition of amino acids in a subunit. The constraints are rules, such as the requirements for close packing and symmetry matching among the virus components, assumed for creating mathematical models. Foremost among the rules is the pitch connection, which relates the lattice constants of mechanically linked, concentric structures with helical and/or rotational symmetry, particularly the DNA and its protein coat.

The modeling procedure generates geometrically feasible models and their theoretical diffraction patterns as functions of trial input symmetry indices. The theoretical patterns are compared to an experimental pattern in order to filter out those models with incorrect symmetry indices. This contrasts with the usual procedure, in which experimental intensities are included as input data for a model. Our procedure has allowed us to find two successful models for Pfl virus, one similar to a model in the literature and the other significantly different from previously proposed models.

**T-PM-Po80** THE ASSOCIATION OF WATER MOLECULES WITH CHROMATIN STRUCTURES WITHIN THE CELL NUCLEUS.

C.F. Hazlewood<sup>1</sup>, and M. Kellermayer<sup>1,2</sup>, Depts. Physiology, Baylor College of Medicine<sup>1</sup>, Houston, TX 77030, and Dept. of Clinical Chem., University Medical School<sup>2</sup>, H-7624, Pécs, Hungary. Gene regulation of eukaryotic cells involves changes in the hydration of chromatin, however, the role(s) of water in this process is not understood. We are attempting to gain insight into the role(s) of water and monovalent ions by studying nuclei isolated from lymphocytes. Nuclei are isolated from bovine thymus glands in a buffered sucrose solution (TSCM) containing a detergent,  $\text{Ca}^{++}$ , and  $\text{Mg}^{++}$ . The morphology of these nuclei is well preserved in that their size and shape is similar to that in the intact cell. The water content of the pelleted nuclei was determined at different centrifugation (g) forces ranging from 1,000 g's to 150,000 g's. Under these conditions it was found that the water content of the nuclei was constant (65%) between 40,000 and 150,000 g's. If the nuclei (isolated in the TSCM solution) are pelleted at a low g force, resuspended in buffered solution containing 15 meq/L  $\text{Na}^+$ ,  $\text{K}^+$ , sucrose,  $\text{Ca}^{++}$  and  $\text{Mg}^{++}$  (i.e. same osmolarity as the TSCM solution), and then centrifuged at different rates, it is found that the percentage of water in the pelleted nuclei is increased by 6-8% (i.e., the "water holding capacity" of the nuclei is increased when monovalent ions  $\text{Na}^+$  and  $\text{K}^+$  are present). When the nuclei are exposed to a buffered solution containing 75 meq/L  $\text{Na}^+$  and  $\text{K}^+$ , the "water holding capacity" is increased by 18-20%. The relaxation times of the water protons in the nuclear pellets were found to be lower than those for pure water but proportional to the water content of the pellets. These results indicate that the monovalent cations may be directly involved in the regulation of chromatin hydration. (This work supported in part by R.A. Welch Found. Q-390, ONR N0004-76-C-0100, and USDA/CNRC).

**T-PM-Po81** NUCLEIC ACID AND PROTEIN SEQUENCE DATABASES. M.O. Dayhoff, B.C. Orcutt, W.C. Barker, L.T. Hunt, H.R. Chen, L.-S. Yeh, and D.G. George. National Biomedical Research Fdn., Georgetown University Medical Center, Washington, D.C. 20007

A dream of research scientists is to think creatively, having data as well as manipulative and computational capability instantly available. Comparative work of any complexity involving nucleic acid and protein sequences requires at least some help from computers. It is our aim to develop systems that aid the creative processes. We will demonstrate the database computer systems. Manipulations of the data are performed on single entries or on "current lists" of entries that have usually been formed by retrieval commands. They include translation of nucleic acid sequences to proteins and reverse translation, searching for hypothetical proteins, searching for particular sequences or enzyme restriction sites, and tabulation of codon usage and the frequency of occurrence of single residues or pairs and triplets. Sequences can be compared and the differences tabulated or displayed in an alignment. Retrieval can be effected by evolutionary hierarchy of the species, by chemical relationships of the sequences, by keywords, and by the sequence itself. One can browse through the material or use the computer equivalents of table of contents, subject and author indexes, taxonomic index, and table of compositions and lengths. Nontraditional items such as the initials of the author, the journal, page number, and year of publication, or any other string of characters from the text or sequences, can also be used for retrieval.

Partially supported by NIH grant GM08710 and NASA contract NASW3317.

**T-PM-Po82** SALT DEPENDENCE OF THE HELIX-TO-COIL TRANSITION OF THE DEOXYRIBOHXANUCLEOTIDE d(CGCGCG)  
Luis A. Marky, Roger A. Jones and Kenneth J. Breslauer, Department of Chemistry, Rutgers University, New Brunswick, New Jersey 08903.

The self-complementary deoxyribohexanucleotide d(CGCGCG) was synthesized by the phosphotriester method. The double strand to single strand transition of this oligomer was thermodynamically characterized by differential scanning calorimetry, temperature-dependent u.v. and circular dichroism spectroscopy.

In 1M NaCl buffer solution the calorimetric experiments provide a value of 50 kcal/mole in double strands for the transition between 5 and 95°C. The spectrophotometric value based on a plot of inverse melting temperature vs. ln of concentration is in good agreement with calorimetry suggesting a two state transition. The results are compared with similar studies of the deoxyribo-nucleotide sequence isomer d(GCGCGC) [Biochemistry 20, 1409 (1981)].

If the salt concentration is changed to 5M a different helix conformation is obtained at low temperatures as seen by the circular dichroism spectra. The transition of this helix to the coil state is also characterized and compared with that in 1M NaCl solution and the thermodynamic results are discussed in terms of specific molecular interactions.

This work was supported by NIH Grant GM-23509.

**T-PM-Po83** FLUORESCENCE STUDIES OF TOMAYMYCIN-DNA ADDUCT, M.D. Barkley and A.T. Swim, Department of Biochemistry, University of Kentucky Medical Center, Lexington, KY 40536. Supported by NIH grant GM22873.

Tomaymycin is a pyrrolo(1,4)benzodiazepine antitumor antibiotic. CPK models predict that these drugs fit snugly in the DNA minor groove, held by an aminal linkage to N-2 of guanine plus secondary hydrogen-bonding interactions (R.L. Petrussek et al., *Biochemistry* 20, 1111-1119 (1981)). The fluorescence of tomaymycin was found to be quite sensitive to environment. In polar solvents and in DNA adducts the fluorescence emission is substantially enhanced and red-shifted. Addition of low concentrations of polar solvents to nonpolar solvents increases the fluorescence of tomaymycin and shifts it to the red. The fluorescence decay of the tomaymycin-DNA adduct and of the free drug in glycerol was observed to be biexponential. These results suggest an excited-state reaction of tomaymycin with its surroundings.

The pH dependence of the fluorescence was also determined. Tomaymycin fluorescence is severely quenched at alkaline pH. The  $pK_a = 8.0$  for the free drug measured by absorption and by fluorescence indicates that the fluorescent species is the neutral excited molecule. The group being titrated in this pH range is probably the phenolic proton on the aromatic ring. No fluorescence quenching is observed for the tomaymycin-DNA adduct until pH = 11.5, where the DNA double helix denatures. Subsequent reduction of the pH restores about 50% of the fluorescence. Since the tomaymycin-DNA adduct is stable under alkaline conditions, this suggests that the phenolic proton is inaccessible to solvent in double-stranded but not in single-stranded DNA. This conclusion is consistent with proposed structures for the tomaymycin-DNA adduct (L. Hurley, personal communication).

**T-PM-Po84**  $\alpha$ -CHYMOTRYPSIN; A TOPOLOGICAL PROBE OF THE NUCLEOSOME CORE

Nancy Rosenberg, The Institute of Molecular Biophysics, Florida State University, Tallahassee, Florida 32306.

$\alpha$ -chymotrypsin, with a molecular weight of 25,000, specific for tyrosine, tryptophan, phenylalanine, and to a moderate degree, methionine and leucine, has been shown to be a good probe of the nucleosome core's topology. High resolution polyacrylamide gel electrophoresis has indicated that  $\alpha$ -chymotrypsin cleaves to a limited and stable extent the core histones at approximately seven accessible sites over a range of 2-160  $\mu$ g enzyme/100  $\mu$ g core histone. Sedimentation studies have demonstrated that digestion is accompanied by unfolding, while concurrent electrophoretic analysis of individual fractions suggests the presence of an intermediate unfolded nucleosomal core species. Circular dichroic spectra have shown that  $\alpha$ -chymotrypsin affects the winding angle of DNA associated with the nucleosome core.

\* The author wishes to acknowledge Dr. Randolph L. Rill for his continual support and research guidance.

**T-PM-Po85**

Abstract rescheduled to M-AM-F11

**T-PM-Po86** MULTI-COMPONENT CHOLINERGIC DESENSITIZATION AT FROG NEUROMUSCULAR JUNCTION AND *APLYSIA*. T.J. Chesnut, N.T. Slater, D.O. Carpenter and C. Edwards (Introduced by M. King), Department of Biological Sciences, SUNY and N.Y. State Department of Health, Albany, New York.

The time courses of desensitization onset and recovery to acetylcholine (ACh) applied by ionophoresis were monitored at voltage-clamped neuromuscular junctions of sartorius muscles of *Rana pipiens*. Semi-logarithmic plots of both the onset and recovery of desensitization displayed two time constants. The time constants for onset were  $10.4 \pm 1.0$  and  $115 \pm 22$  sec., while for recovery they were 9.7 and 325 sec. Application of metabolic inhibitors (0.25 mM 2,4-dinitrophenol and 0.1 mM 1-fluoro,2,4-dinitrobenzene) decreased the slower time constant of desensitization onset, while increased ACh dose selectively decreased the faster time constant of desensitization onset. The application of metabolic inhibitors also depressed the early stages of recovery from desensitization, probably by an effect on the faster component of recovery. The effects of agonist dose were tested by adjusting the ionophoretic current to obtain a desired response amplitude. The effects of agonist dose appeared to be dependent on the concentration of calcium ions in the Ringer, being more selective at lower calcium concentrations. The onset of desensitization of  $\text{Na}^+$ -mediated responses to ionophoretic application of ACh on voltage-clamped *Aplysia* RB neurons also displayed two time constants ( $17.2 \pm 2.0$  and  $118.2 \pm 46.6$  sec.). The data from both preparations are consistent with the hypothesis that at least two independent processes are involved in the mechanism of desensitization. (Supported by NIH grants NS 0781 to C.E. and F32NS06440 to N.T.S.)

**T-PM-Po87** STRYCHNINE BLOCKADE OF EXCITATORY ACETYLCHOLINE RESPONSES IS NOT VOLTAGE DEPENDENT. N.Traverse Slater\* and David O.Carpenter, Division of Laboratories and Research, New York State Department of Health, Albany, N.Y. 12201.

Recent evidence has suggested that the blockade of both neuronal and neuromuscular excitatory responses to acetylcholine (ACh) by some "classical" antagonists may occur by a blockade of the open receptor-ionophore complex (RIC), probably by a blockade of the ionic channel. In these experiments we have studied the voltage dependence of the blockade produced by strychnine, hexamethonium and atropine of the inward currents evoked by ACh and carbachol on voltage-clamped RB cell somata in *Aplysia* abdominal ganglia. Agonists were applied by ionophoresis and antagonists were applied by bath perfusion. Agonist-evoked currents were measured over a range of membrane potentials (-60 to -120 mV) using the sequential voltage jump method described by Ascher, Large and Rang<sup>1</sup>, whereby steady-state agonist-evoked currents can be measured at equilibrium concentrations of both agonist and antagonist. Both hexamethonium and atropine antagonized responses to ACh and carbachol in a voltage-dependent manner, the degree of blockade increasing with hyperpolarization. The antagonism of responses to ACh and carbachol by strychnine, however, was not voltage-dependent, the degree of blockade being equal at all membrane potentials studied. This difference between the voltage dependencies of these drugs suggests a difference in the site of action of these drugs: blockade by strychnine may result from an interaction with the closed state of the RIC (possibly the receptor), and blockade by hexamethonium and atropine may result from an interaction with the open state of the RIC (possibly the ionic channel).

<sup>1</sup> Ascher, P., Large, W.A. and Rang, H.P. (1979) *J. Physiol.* 295:139-170.

**T-PM-Po88** SPONTANEOUS HYPERPOLARIZATIONS IN CULTURED BULLFROG GANGLION CELLS REFLECT K-CHANNELS OPENED BY INTERNAL CALCIUM PACKETS. P. R. Adams, D. A. Brown, A. Constanti and C.E.Y. Adams, Department of Neurobiology, S.U.N.Y. Stony Brook and Department of Pharmacology, School of Pharmacy, London, U.K.

Approximately half of neurons impaled in cultured bullfrog ganglion explants exhibited random spontaneous hyperpolarizing events, similar to those recently reported for dorsal root ganglion cells by Mathers and Barker (Br. Res. 211, 451). Under voltage clamp these events manifested as spontaneous miniature outward currents (s.m.o.c.s) with abrupt risetimes ( $\sim 3$  msec) and exponential decays (8 msec at -40 mV). Depolarizing the cell increased the s.m.o.c. amplitude and frequency, and reduced the decay rate, to about 20 msec at 0 mV. To test the hypothesis that a s.m.o.c. is due to emptying of a small calcium packet near the inner membrane surface, we injected calcium into the same cell iontophoretically, and performed voltage jump relaxation experiments on the calcium-activated K current ( $I_K$ ). The time constants of the s.m.o.c. decay and the  $I_K$  relaxations were similar in the potential range -40 to +20 mV. Furthermore voltage jumps applied during s.m.o.c. decays or Ca-injection elicited relaxations with similar time constants. It is concluded that a s.m.o.c. reflects the liberation of a calcium packet with 0.1  $\mu\text{m}$  of the inner membrane surface, opening 10 to 5000  $I_K$  channels. Calcium is rapidly sequestered, so that the s.m.o.c. decay reflects the lifetime of the  $I_K$  channels.

Supported by NS14986, NS15846 and the Klingenstein Foundation.

**T-PM-Po89** LATERAL DIFFUSION OF LIGAND-FREE ACETYLCHOLINE RECEPTORS *IN VIVO* MEASURED BY LOCAL INACTIVATION RECOVERY. S.H. Young and M-m. Poo, Dept. of Physiology & Biophysics, UCI, Irvine, CA 92717

Although measurements of lateral diffusion of membrane proteins have been carried out in a number of *in vitro* preparations, it is not clear whether membrane proteins are capable of lateral diffusion within intact tissue. Here we report a study of lateral diffusion of acetylcholine receptors (AChRs) in the myotomal membrane of *Xenopus* tadpole by a newly developed technique of local inactivation recovery.

The myotomal fiber surface of *Xenopus* tadpoles was exposed to external solution by gently removing the skin of the tail. The density of AChRs was monitored by membrane depolarizations in response to iontophoretically applied pulses of ACh. A pulse of  $\alpha$ -bungarotoxin was pressure ejected onto the exposed fiber surface, resulting in a rapid local inactivation of AChRs. With time, the ligand-free AChRs diffused into the region of inactivation, producing a recovery of ACh sensitivity. That the observed recovery of ACh sensitivity is due to diffusion of AChRs from the unexposed under-surface of the fiber to the inactivated region was evidenced by the following: 1) No recovery was observed following prolonged toxin application. 2) Pre-treatment with Concanavalin A, which cross-links and immobilizes AChRs, prevents recovery. 3) Mapping of ACh sensitivity along the fiber axis shows no significant longitudinal component of diffusion. 4) The diffusion coefficients observed after scaling the recovery rate with fiber diameter fell within a small range ( $1-4 \times 10^{-9} \text{ cm}^2/\text{s}$ ), consistent with diffusion of AChRs around the fiber perimeter. This finding of rapid lateral diffusion of AChRs *in vivo* supports the notion that a simple diffusion-trap mechanism could account for the localization of AChRs during synaptogenesis. (Supported by NSF grant BNS-8012348.)

**T-PM-Po90** CHARACTERIZATION OF CHOLINERGIC AGONIST PROPERTIES FOR A NEW FLUORESCENT (NBD)-BISQUATERNARY LIGAND. Michael B. Bolger, Vincent E. Dionne, and Palmer Taylor, USC School of Pharmacy, Los Angeles, CA, 90033 and UCSD Division of Pharmacology La Jolla, CA, 92093

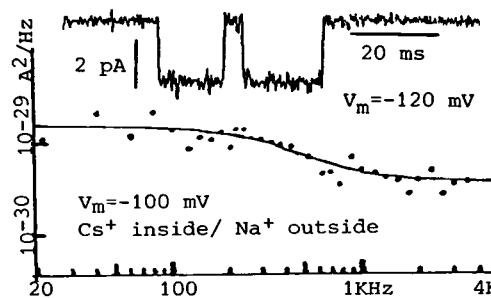
Introduction of a relatively hydrophobic fluorophore at the acyl end of choline analogs has generally produced cholinergic ligands with some antagonist or local anesthetic properties. In an attempt to optimize agonist properties by enhancing ligand polarity we have prepared a fluorescent analog of suberyldicholine. Incorporation of a 4-nitrobenzo-2-oxa-1,3-diazole (NBD) fluorophore at the secondary nitrogen of 3,3'-iminodipropionylcholine has provided a fluorescent ligand (4-(bis(choline)-3',3'-iminodipropionyl)-7-nitrobenzo-2-oxa-1,3-diazole, BCNI) that does exhibit cholinergic agonist properties. Pre-steady state carbamylation of acetylcholinesterase by 7-(dimethylcarbamoyloxy-N-methylquinolinium iodide (M7C) is subject to competitive inhibition ( $\text{IC}_{50}=0.5-1 \mu\text{M}$ ) by BCNI. Binding of [ $^{125}\text{I}$ ]- $\alpha$ -toxin to isolated acetylcholine receptor (AChR) containing membrane fragments from *Torpedo* is inhibited by BCNI ( $\text{IC}_{50}=0.1 \mu\text{M}$ ) following equilibrium (30m) prior exposure to increasing amounts of the fluorescent ligand. When BCNI and [ $^{125}\text{I}$ ]- $\alpha$ -toxin are added simultaneously, the dose response curve for inhibition is shifted to the higher concentrations ( $\text{IC}_{50}=1 \mu\text{M}$ ). Thus, prior exposure to BCNI produces an increase in the apparent affinity of AChR for this fluorescent ligand. Similar observations for classical cholinergic agonists such as carbamylcholine previously have been correlated with the process of agonist-mediated receptor desensitization. Electrophysiological studies of the snake neuromuscular junction support the agonist-like classification of this compound. Analysis of noise resulting from iontophoretic application of BCNI to a single endplate results in a complex power spectrum which indicates that BCNI can induce channel open times of 1-2 ms and a single channel conductance of 25-35 psemes.

**T-PM-Po91** FLUCTUATIONS IN THE CURRENT THROUGH OPEN ACh-RECEPTOR CHANNELS. F.J. Sigworth, Max-Planck-Institut für Biophys. Chem., Göttingen, F.R.G.

Acetylcholine-activated single channel currents, recorded from rat myoball membranes at low temperature ( $8^\circ$ ) and high resolution, show more noise when a channel is open than when it is closed. Fluctuations in ion flow would be expected from shot noise or  $1/f$  noise mechanisms; surprisingly, however, neither seems to predominate in the frequency range studied here.

The difference spectrum, computed from portions of records with channels open and with channels closed, can be fitted by a low-frequency Lorentzian ( $f \approx 300 \text{ Hz}$ , corresponding to  $\tau \approx 0.5 \text{ ms}$ ) plus a constant high-frequency component having  $\sim 4$  times the spectral density expected for shot noise. The low-frequency component is especially intriguing since no gating process occurs on this time scale (mean channel open time is 50 ms under these conditions), and it appears not to arise from step-wise changes in channel conductance.

Ps. 118:23



**T-PM-Po92** DOUBLE-EXPONENTIAL CHANNEL CURRENT LIFETIME DISTRIBUTIONS IN CULTURED NERVE AND MUSCLE. (Meyer B. Jackson, Biology Dept., UCLA and Harold Lecar, Laboratory of Biophysics, NINCDS, NIH).

The kinetics of closing of chemically activated channels were examined using single channel current recording techniques. Acetylcholine receptor channels in cell cultures of rat, human, and chick muscle, as well as GABA receptor channels in mouse spinal cord, were studied. In all four preparations, channel open-state lifetime distributions were found to deviate from a single exponential function. Curve fits to single exponential functions and sums of two exponentials were compared. The double exponential function produced fits of much higher quality. The data is tentatively interpreted as having two kinetic components with different characteristic relaxation times. The faster relaxation time is often close to the limiting instrumental time response. Distortions due to the system bandwidth would produce a deficit of fast events but the fast process is manifest as an excess of fast events. Previous studies of current noise failed to resolve the faster process. Since slower processes contribute more power per unit bandwidth to a power spectrum, noise analysis weights faster processes unfavorably. Noise generated by an equal number of fast and slow events is dominated by the slower process.

The mechanism underlying the closing transition is not uniquely determined by the open-state lifetime distribution, but the result indicates that the channel closing process is more complicated than previously thought. Furthermore, the widespread observation of this phenomenon suggests that it is an important aspect of chemosensitivity.

**T-PM-Po93** MUSCARINE (MUS) DECREASED A VOLTAGE-DEPENDENT POTASSIUM CURRENT IN MOUSE SPINAL CORD NEURONS IN CELL CULTURE. L.M. Nowak and R.L. Macdonald (Intr. by D.C. Dawson, Dept. of Physiol.) Dept. of Neurology, U. of Michigan, Ann Arbor, MI 48109.

We have investigated the postsynaptic mechanism of MUS action on cultured mouse spinal cord neurons and report that MUS decreased a voltage-dependent potassium current which was present at resting membrane potential. Spinal cords and attached dorsal root ganglia were dissected from 12-14 day old fetal mice and grown in culture by conventional methods for 4-10 weeks prior to electrophysiological investigation. A single electrode voltage-clamp procedure was used to measure MUS induced current and voltage-jump induced current relaxations. MUS evoked inward current which decreased with hyperpolarization and reversed polarity near potassium equilibrium potential ( $E_K$ ). Reversal potential varied as a linear function of the log of extracellular potassium concentration. Steady state current-voltage relationships generated by injecting variable amplitude, hyperpolarizing and depolarizing voltage-command pulses in control and MUS-containing solutions revealed that MUS decreased membrane conductance. The conductance decrease was greater with depolarizing commands suggesting that MUS reduced a V-dependent potassium current which was activated by depolarization. Brief (0.5-1sec) hyperpolarizing commands (0 to -80 mV) were applied from holding potentials between -15 and -45 mV. Small V-steps evoked instantaneous currents followed by inward current relaxations. Large V-commands evoked outward current relaxations below  $E_K$ . Current relaxations were reduced in amplitude by MUS but not tetraethylammonium. Thus, MUS decreased a time and V-dependent potassium current ( $I_M$ ) similar to that described in frog sympathetic ganglion neurons (Brown & Adams, 1980). NIH supported: NS15225, NS00408, NS06791.

**T-PM-Po94** VOLTAGE JUMP RELAXATION EXPERIMENTS ON THE CHEMICALLY-MODIFIED ACETYLCHOLINE RECEPTOR. A. Steinacker and \*D.C. Zuazaga. Biophysics, The Rockefeller University, New York, N.Y. 10021 & \*Lab. of Neurobiology, Univ. of Puerto Rico, San Juan, P.R. 00901

Modification of the acetylcholine receptor (AChR) protein by sodium bisulfite, a reagent which sulfonates the disulfide bonds associated with acetylcholine (ACh) binding sites, changes the functional properties of the receptor. We have used a three-state kinetic model ( $A+R \rightleftharpoons AR \rightleftharpoons AR^*$ ) to explain the observed increase in miniature endplate current (mepc) decay time without a corresponding change in single channel open time, as measured by noise analysis, and proposed that it is the time spent in the intermediate bound but not open state (AR) what is increased after bisulfite modification of the AChR at the lizard neuromuscular junction (Steinacker & Zuazaga, PNAS, in press). The theoretical framework provided by Colquhoun and Hawkes (Proc. Roy. Soc. Lond. B. 199: 231, 1977) shows this to be theoretically possible and states that voltage jump relaxation experiments should also reflect predominately the lifetime of the occupied state. Voltage jump current relaxation experiments were performed and the time constants obtained after bisulfite modification were found to be 50-75% longer than control values. These findings support our hypothesis that bisulfite modification increases the time ACh is bound to the receptor before the channel opens.

Supported by Muscular Dystrophy Association and NIH NS 15956(A.S.) and NIH NS 07464 (D.C.Z.).

**T-PM-Po95** THE KINETICS OF LOCAL ANESTHETIC BLOCKADE OF END-PLATE CHANNELS. R. L. Ruff. Dept. of Physiology & Biophysics, U. of Washington, Seattle, WA.

The effect of the local anesthetic QX222 on the kinetics of miniature end-plate currents (MEPC's) and acetylcholine induced end-plate current fluctuations was studied in voltage clamped frog cutaneous pectoris neuromuscular junctions. The rate constants for end-plate channel closure, blockade by the local anesthetic molecule, and removal of the local anesthetic molecule from the channel were calculated from the MEPC decay parameters according to a kinetic scheme in which a single positively charged local anesthetic molecule enters and blocks an open end-plate channel (Ruff, J. Physiol. 264:89-124, 1977). The channel closing rate was not affected by 0.1 or 0.2 mM QX222. At 18°C the blocking rate constant was  $1.1 \pm 0.3 \times 10^7 \exp(-0.009 \pm 0.003 \times V) \text{ sec}^{-1} \text{ M}^{-1}$ , and the unblocking rate constant was  $5.7 \pm 0.6 \times 10^2 \exp(0.011 \pm 0.002 \times V) \text{ sec}^{-1}$ . The dissociation constant was close to 10  $\mu\text{M}$  at -80mV. End-plate fluctuations indicated that QX222 lowered the effective single channel conductance suggesting a finite blocked state conductance of 1.6pS. For the iontophoretically produced current, the end-plate current variance was linearly proportional to the mean current which suggests that the reduction in the single channel conductance did not result from a reduction in the population of end-plate channels that can open. Increasing the low-pass filtering frequency to 20KHz did not change the value of the effective single channel conductance. It is possible, however, that a rapid fluttering of the local anesthetic molecule at its binding site at a rate > 20KHz could have resulted in an apparent reduction of the single channel conductance. Supported by NIH#NS00498, NS16696.

**T-PM-Po96** SITE-SPECIFIC FLUORESCCEIN ISOTHIOCYANATE-LABELED  $\alpha$ -COBRA TOXIN: BIOCHEMICAL AND SPECTROSCOPIC CHARACTERIZATION. David A. Johnson and Palmer Taylor\*, Division of Pharmacology, Department of Medicine, University of California at San Diego, La Jolla, California 92093

Cobra  $\alpha$ -toxin purified from *naja naja siamensis* venom was labeled with near stoichiometric quantities of fluorescein isothiocyanate (FITC). A mono-fluorescein  $\alpha$ -toxin was separated with a yield of 50-60% from unconjugated  $\alpha$ -toxin and other reaction products by ion exchange chromatography. The isolated monoconjugated  $\alpha$ -toxin electrofocuses largely as a single entity with  $\sim 93\%$  appearing with a pI  $\approx 9.55$ . The corresponding value for native toxin is 10.77. Thermolysin digestion and high pressure liquid chromatography of the resultant peptides yield two dominant fluorescent peaks, both of which can be traced to the labelling of lysine 23. The N<sup>F</sup>-FITC-lysine-23  $\alpha$ -toxin shows a reduced quantum yield when compared with free FITC or the denatured and reduced FITC- $\alpha$ -toxin. The reduction of fluorescence is likely due to interactions between the fluorescein and trp-25 and/or tyr-21 residues in the  $\beta$ -sheet region of the toxin. Binding of the N<sup>F</sup>-FITC-lys-23  $\alpha$ -toxin to the *Torpedo californica* acetylcholine receptor causes an  $\sim 80\%$  increase in fluorescence which probably reflects a perturbation of the  $\beta$ -sheet structure of the 20-25 residue region of the  $\alpha$ -toxin. Fluorescein  $\alpha$ -toxin binds to the acetylcholine receptor with a dissociation constant of  $\sim 4 \text{ nM}$ . Steady state fluorescence polarization measurements of N<sup>F</sup>-FITC-lys-23  $\alpha$ -toxin yield a rotational correlation time of  $\sim 3.7 \text{ nsec}$ , a value consistent with the overall dimensions of the  $\alpha$ -toxin molecule, thus, independent molecular motion of the conjugated fluorescein is not detectable. The N<sup>F</sup>-FITC-lys-23  $\alpha$ -toxin is being used in conjunction with reversible fluorescent agonists and antagonists to assess the intersite distances on the receptor.

**T-PM-Po97** IONIC DEPLETION AND VOLTAGE GRADIENTS AT THE ENDPLATE

H. Jachter and F. Sachs, Dept. of Biophysics, SUNY, Buffalo, N.Y. 14214

We have constructed a computer model of the miniature end plate current (mepc) using a four state sequential model in a 2 dimensional disk geometry similar to that presented by Adams (1). In addition to Ach diffusion, we have included ionic depletion/accumulation of both Na<sup>+</sup> and K<sup>+</sup> ions, with consequent changes in resistivity, voltage gradients and reversal potential as modeled by the Goldman equation. We have used a method whereby the inhomogeneous diffusion equation with forcing function is integrated by decomposing it into its analytically obtained homogeneous and numerically evaluated inhomogeneous parts. Using this method it was possible to run a 10 msec simulation on a mini-computer in less than 30 min.

Results indicate that at a potential of -90mV an mepc can produce Na<sup>+</sup> depletion exceeding 70% near the site of release. Similarly K<sup>+</sup> accumulation in the cleft can exceed 300% of normal at potentials as negative as -40mV. An elevation of this magnitude may could potentially modulate transmitter release. At -90mV the voltage gradient from the release site may be 15mV. These simulations support Attwell and Iles (2) contention that the mepc kinetics are significantly diffusion controlled.

Currently, we are using this model to examine the effects of solution viscosity, receptor density, ionic concentrations, voltage dependent kinetics and esterase activity on the mepc.

(1) Information Processing in the Nervous Sys. Pinsker and Willis Ed. Raven Press (1980)

(2) Proc. R. Soc. 209, 115-31 (1979)

**T-PM-Po98** DIVALENT CATION EFFECTS AT ENDPLATE CHANNELS C. A. Lewis, Dept. Biophysics, SUNYAB 118 Cary, Main St. Campus, Buffalo, NY 14214

$\text{Ca}^{++}$  is a permeant cation through endplate channels, so increasing  $(\text{Ca})_o$  would be expected to increase the depolarization of the reversal potential. Endplates on the cutaneous pectoris muscle from northern *Rana pipiens* were voltage clamped with two microelectrodes. ACh was iontophoretically applied, and the reversal potential was determined by interpolation of the ACh-induced endplate current versus voltage relationship. Experiments were performed in Ringer's solutions containing 50% normal Na (57.5 mM) and Ca concentrations ranging from 2 to 40 mM with sucrose being added to maintain osmolarity. Increasing the external Ca concentration from 2 to 5 mM caused the reversal potential to become depolarized, while increasing the Ca concentration still higher resulted in more hyperpolarized reversal potentials. This same effect was seen with Ni as the divalent cation. The simple Goldman-Hodgkin-Katz reversal potential formulation with a fixed, negative surface charge density cannot explain all of these measurements.

**T-PM-Po99** CURRENT- AND VOLTAGE-DEPENDENT BLOCK OF ACETYLCHOLINE-ACTIVATED IONIC CHANNELS BY GUANIDINE DERIVATIVES. S. Vogel and T. Narahashi, Dept. of Pharmacology, Northwestern Univ. Med. School, Chicago, IL 60611.

The alkyl derivatives of guanidine are suggested to block the acetylcholine-activated ionic channel. To further examine the drug-channel interaction, frog cutaneous pectoris muscles were voltage clamped by the two-microelectrode technique. Clamp steps from a holding potential of -60 mV lasted for 5 sec, and the end-plate current (epc) was elicited by nerve stimulation at 3 sec. Both octylguanidine ( $\text{C}_8$ ), at 5  $\mu\text{M}$ , and ethylguanidine ( $\text{C}_2$ ), at 3 mM, depressed inward epc's more markedly than outward epc's. In  $\text{C}_8$ , block was not influenced by repetitive nerve stimuli at frequencies between 0.1 and 1.0 Hz either at -60 mV or at +40 mV. Test currents elicited 100 msec after a 5 sec voltage prepulse were increased by a depolarizing prepulse (e.g., to +40 mV) and decreased by a hyperpolarizing prepulse (to -80 mV). Conditioning stimuli applied at 1.0 Hz during these prepulses had no effect on test currents beyond that caused by the prepulse alone. These results suggest that  $\text{C}_8$  binds to the closed channel in a voltage-dependent manner. In contrast to  $\text{C}_8$ ,  $\text{C}_2$  block of the epc was influenced by repetitive stimuli. At -60 mV, stimulation at frequencies between 0.1 and 1.0 Hz enhanced  $\text{C}_2$  block of the inward epc. Steady-state block was achieved with 5-7 stimuli and was independent of the frequency. At +40 mV, repetitive stimuli relieved block of the outward epc, again in a frequency-independent manner. These findings suggest that block caused by  $\text{C}_2$  is influenced by the direction of current flow through open channels. Hence, short-, but not long-chain guanidine derivatives exhibit current-dependent block. Supported by NIH grant NS 14145.

**T-PM-Po100** PERMEABILITY CHANGES INDUCED BY L-GLUTAMATE AT THE CRAYFISH NEUROMUSCULAR JUNCTION. M.S. Dekin\*, C. Edwards, and A.R. Freeman. Neurobiology Research Center, SUNY at Albany, 1400 Washington Avenue, Albany, N.Y. and Department of Physiology, Temple University School of Medicine, N. Broad Street, Philadelphia, PA.

The permeability changes at the voltage-clamped crayfish neuromuscular junction induced by ionophoretically applied L-Glutamate were studied. Muscles were bathed for 1 hr in a solution in which 50% of the  $\text{Na}^+$  was replaced by tetrabutylammonium; this treatment irreversibly increases membrane resistance and blocks contraction (Fatt and Katz, *J. Physiol. Lond.*, 120, 1953). The reversal potential ( $V_r$ ) of these muscles in normal Van Harreveld's solution measured by interpolation was  $+6.3 \pm 2.1$  mV ( $n = 15$ ). The effects of changes in the ionic composition of the bathing solution were also studied. A 10 fold reduction in  $\text{Ca}^{++}$  and  $\text{Mg}^{++}$ , adding sucrose to keep the osmolarity constant, shifted  $V_r$  to  $+5.5 \pm 3.1$  mV ( $n = 12$ ). Isotonic replacement of  $\text{Na}^+$  by  $\text{K}^+$ ,  $\text{Ca}^{++}$ , and  $\text{Mg}^{++}$  resulted in the following  $V_r$ 's:  $+7.4 \pm 1.2$  mV ( $n = 4$ ) for  $\text{K}^+$ ,  $-22.4 \pm 3.4$  mV ( $n = 7$ ) for  $\text{Ca}^{++}$ , and  $-19.7 \pm 3.2$  mV ( $n = 5$ ) for  $\text{Mg}^{++}$ . The dependence of  $V_r$  on mixtures of  $\text{Na}^+$  and  $\text{K}^+$  was also studied and it followed the relationship predicted by the constant field equation. The relative permeability ratio,  $P_x/P_{\text{Na}}$ , can be estimated from the shift in  $V_r$  for the substituted solutions. The calculated  $P_x/P_{\text{Na}}$ 's for  $\text{K}^+:\text{Na}^+:\text{Mg}^{++}:\text{Ca}^{++}$  were 1.1:1:.51:.43 respectively. These data show that L-Glutamate causes a non-specific increase in membrane permeability to cations. (Supported by NIH grant NS 0781)



**T-PM-Po101 THE EFFECT OF PHOTOISOMERIZABLE AGONISTS ON FISH MUSCLE.** Martin Weinstock, Division of Biology, California Institute of Technology, Pasadena, CA 91125

Muscle fibers of the African knife fish (*Xenomystus nigri*) were voltage clamped at -75 mV (temperature = 10°C) in a bathing medium containing 10 - 100 nM cis-Bis-Q, a photoisomerizable molecule which does not act as an agonist at the nicotinic receptor. A flash of light converted some cis-Bis-Q to trans-Bis-Q, which is an agonist. The resulting agonist-induced current reached a maximal value after several seconds. This relatively slow increase (compared with similar experiments at Electrophorus electroplaques) may indicate a significant diffusion delay in the interaction of agonist molecules in the bath with their receptors. The elementary channel properties of the trans-Bis-Q activated channel were calculated from an autocorrelation analysis of current noise. The trans-Bis-Q activated channel has a conductance of  $31 \pm 6$  pS (mean  $\pm$  S.D.) and a mean lifetime of  $3.6 \pm 1.0$  msec. For comparison, ACh was iontophored onto the fish neuromuscular junction under voltage clamp conditions and the resulting current noise was analyzed. The ACh activated channel has a conductance of  $25 \pm 4$  pS and a mean lifetime of  $3.5 \pm .4$  msec. Thus, the trans-Bis-Q activated channel is similar to the ACh activated channel.

A second light flash caused a rapid, transient decrease, similar to phase 1 at Electrophorus electroplaques, followed by a further sustained increase in agonist induced current; after several flashes, the steady holding current increased no further. Light flashes after this point caused, in addition to phase 1, temporary increases in current that decayed within seconds. This temporarily increased current rise may represent a partial recovery from desensitization caused by trans to cis conversion of agonist bound to desensitized receptor, thus allowing the receptor to regain its sensitivity. Supported by Muscular Dystrophy Association of America and NS-11756.

**T-PM-Po102 SINGLE CHANNEL RECORDING OF WEAK CHOLINERGIC AGONISTS.** Harold Lecar, Catherine E. Morris\* and Brendan S. Wong, NINCDS, NIH, Bethesda, MD 20205.

Single channel studies of drug-activated channel current show that different cholinergic agonists produce different mean channel open time. In general, stronger agonists give longer mean open time. There are cholinergic compounds, however, which are not only especially weak agonists, but also have a blocking action on the receptor. The kinetics of single channel current jumps were studied in order to develop a unified model for antagonists, depolarizing blockers, weak agonists and strong agonists. Single channel currents were recorded with d-tubocurarine, choline, decamethonium, succinylcholine, carbachol and suberyldicholine in cultured rat myotubes. All these drugs produce channel currents of similar amplitude. In our hands, different rat myotube cultures gave channel conductances of either 32 pS or 48 pS, but very seldom a mixture, regardless of the agonist used. For the cultures used in these experiments, the smaller type was seen almost exclusively. All the drugs produced open-time histograms which can be fit by two exponentials. The slower component ranged from approximately 2 ms for curare to 14 ms for suberyldicholine. The faster component did not vary significantly among the different drugs; values ranged between 0.25 to 0.7 ms, which is close to the limiting time resolution of our detection system. Our experiments show that kinetic factors, and not altered channel amplitude determine the strength of agonist action.

(C.E.M. was supported in part by a grant from the Scottish Rite Foundation. C.E.M.'s present address is Dept. of Biology, University of Ottawa, Ottawa, Ontario, Canada).

**T-PM-Po103 THE AUTOCOVARANCE SPECTRUM FOR A CHEMICAL REACTION SYSTEM WHICH EXHIBITS MULTIPLE STEADY STATES.** V. T. Kurtz. Department of Biophysical Sciences, SUNY at Buffalo, 118 Cary Hall, Buffalo, New York 14214.

A description of the stochastic nature of chemical reactions gives rise to interesting time behaviors, such as transitions among multiple stable steady states, when the dynamical equations of motion contain nonlinearities and the reaction system is held far from equilibrium. Here the fluctuations are usually described by a set of linear equations; the study of these equations involves finding their eigenvalues and eigenvectors. If one considers only reactions which involve a single fluctuating chemical species and which change the population size by one molecule, then it readily demonstrated that the eigenvalue spectrum is real; in addition, the contribution of each eigenmode to the autocovariance function, a convenient measure of the time behavior of a system which exhibits fluctuations, is easily calculated from the corresponding eigenvector. The separate study of a linear reaction and of one which is nonlinear reveals several dramatic differences between the two eigenvalue spectra, their dependence upon the size of the system, and the relative contributions of the various eigenmodes to the autocovariance function. When these two reactions are coupled, the autocovariance spectrum depends upon their relative strength; it can be linear-like, nonlinear-like, or, more interestingly, intermediate between these two extremes. It is in this last domain that it is possible for the system to exhibit multiple steady states. When this is indeed the case, there is only one eigenmode which describes the fluctuations between the two stable steady states; its contribution to the autocovariance spectrum is anywhere from very weak to very strong, depending primarily upon the relative stability of the two stable steady states.

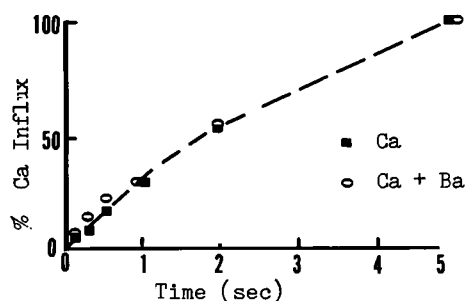
**T-PM-Pol104** EFFECTS OF POLYARGININE ON GATING CURRENT OF SQUID SODIUM CHANNELS. Chau H. Wu and Jay Z. Yeh, Department of Pharmacology, Northwestern University, 303 E. Chicago Avenue, Chicago, Illinois 60611.

Poly-L-arginine with a molecular weight of 60,000 daltons has been shown to block sodium channels preferentially when applied internally to the squid axons (Wu, *Biophys. J.* 33: 208a). The experimental results indicate that the synthetic polypeptide blocks sodium conductance by interacting with the gating moiety of sodium channel at the inner surface of axon membrane and preventing its transition to the open conformation. The hypothesis may be directly tested by examining the effects of polyarginine on the sodium channel gating current. Gating currents were recorded in internally perfused squid axons with the P/4 pulse protocol (Armstrong and Bezanilla, *J. Gen. Physiol.* 63: 533). Both ON and OFF gating currents were reduced by the polypeptide in a dose-dependent manner. The reduction of ON gating current correlated well with the degree of block in sodium current when both the gating and ionic currents were recorded simultaneously in the same axon. We did not detect any significant changes in either the kinetics of ON gating current or the time course of charge immobilization. Thus the results of gating current experiments are consistent with the view that polyarginine binds to sodium channels and hinders the movement of gating charge.

(Supported by NIH grants GM 24866 and NS 14144 and a research grant from Epilepsy Foundation of America.)

**T-PM-Pol105** THE INITIAL TIME-COURSE OF Ca INFLUX IN SYNAPTOSOMES. D.A. Nachshen, Dept. Physiology, University of Maryland, School of Medicine, Baltimore, Md. 21201

Voltage-dependent  $^{45}\text{Ca}$  influx in synaptosomes (isolated presynaptic nerve terminals) from rat brain occurs through inactivating and non-inactivating Ca channels. The time-course of Ca influx through these channels was determined using a Durrum-133 Multi-Mixer, having a time resolution of less than 30 msec. In control experiments, the Ca influx measurement at long times (1-10 sec) was similar with both the conventional (hand-pipetting) and rapid-mixing techniques; this shows that the rapid-mixing procedure does not disrupt the synaptosomes, making them leaky to Ca.



La (0.2  $\mu\text{M}$ ), a highly selective blocker of inactivating Ca channels, abolished the initial, rapid phase of Ca influx, seen in control solutions with 0.02 mM Ca. After the addition of La, the rate of Ca influx was constant for up to 10 sec. Ba (10 mM) had no significant effect on the initial time-course of Ca influx, but reduced the magnitude of the Ca influx by nearly 80%. These results indicate that initial rates of voltage-dependent Ca entry can be studied in mammalian CNS nerve terminals, with a rapid-mixing procedure. Supported by NIH grant NS-16461.

**T-PM-Pol106** INTERNAL pH AFFECTS LIDOCAINE FREQUENCY DEPENDENT BLOCK OF NODE OF RANVIER SODIUM CHANNELS. Joan J. Kendig, Dept. of Anesthesia, Stanford University School of Medicine, Stanford, CA 94305.

In muscle, local anesthetics can be protonated and deprotonated on a sodium channel binding site by changes in external but not internal pH. In the node of Ranvier, barbiturate frequency dependence is enhanced by increasing internal pH and thus the ratio of charged anion to neutral acid. Changes in external pH have little effect. Because muscle and nerve sodium channels may be different, it was of some interest to examine the effect of internal and external pH changes on lidocaine sodium channel block in the voltage clamped node of Ranvier from *Xenopus* sciatic nerve. Axons were subjected to well-buffered solutions of pH 5.5-9.5 externally and at the cut internodes. Diffusion of buffer from the cut ends effectively changes axoplasmic pH at the node. Lowering the pH on either side of the membrane while the pH on the other side was held constant slowed and intensified the frequency-dependent characteristics of lidocaine sodium channel block. Thus the local anesthetic receptor site in nodal sodium channels is accessible to both extracellular and axoplasmic hydrogen ions. The lidocaine cation binding site differs from the barbiturate anion binding site in accessibility to external hydrogen ions, and is effectively nearer the extracellular end of the sodium channel. The lidocaine receptor site in the node is apparently more accessible to axoplasmic protons than that in skeletal muscle, and is effectively nearer the axoplasm. Muscle and nerve sodium channels thus differ in some aspects of their configuration. Supported by NIH Grant GM22113.

**T-PM-Po107** PROPERTIES OF POTASSIUM CHANNELS IN SYNAPTOSOMES. Mordecai P. Blaustein and Regina K. Ickowicz\*. Dept. of Physiology, Univ. of Maryland Medical School, Baltimore, MD 21201.

The properties of nerve terminal K channels were studied by measuring  $^{86}\text{Rb}$  efflux from rat brain synaptosomes (pinched-off presynaptic terminals). The study was based on evidence that K channels are also permeable to Rb (e.g. Reuter & Stevens, 1980, *J. Membrane Biol.* 57: 103). Synaptosomes were loaded at 30°C for 30 min in physiological saline (145 mM Na, 5 mM K) with tracer  $^{86}\text{Rb}$ . The suspensions were then diluted 40-fold into "efflux solutions" which had various K concentrations (Na + K = 150 mM).  $^{86}\text{Rb}$  efflux into control (5 mM K) solution was about 0.2% per sec. When the solution contained 60 mM K, there was an initial rapid  $^{86}\text{Rb}$  efflux of about 5-15% per sec; the efflux then declined to a steady 1-2% per sec within the first few sec, perhaps because of K channel inactivation. Both the rapid initial efflux and the later steady efflux into K-rich solution were blocked by several known K channel blockers including 3,4-diaminopyridine (DAP) (100  $\mu\text{M}$ ) and tetraethylammonium (TEA) (25-50 mM). The magnitudes of both the initial burst and the later steady  $^{86}\text{Rb}$  effluxes were graded functions of  $[\text{K}]_{\text{out}}$ . Efflux was also promoted by depolarizing the synaptosomes with veratridine (50  $\mu\text{M}$ ) + sea anemone toxin (2  $\mu\text{M}$ ); this, too, was blocked by DAP. The K-stimulated  $^{86}\text{Rb}$  efflux was reduced by 1/3 when external Ca was deleted. This suggests that some of the K channels are Ca-activated. Several agents (but not DAP or TEA) blocked K-stimulated  $^{86}\text{Rb}$  efflux with biphasic dose-response curves:  $\text{Ba}^{2+}$ ,  $\text{La}^{3+}$ , quinine  $\text{SO}_4$ , and the psychotomimetic drug, phencyclidine (PCP). These data imply that there are at least two classes of K channels with very different affinities for these agents. (supported by NIH).

**T-PM-Po108** LOW pH MODULATES Na CHANNEL GATING CURRENTS IN FROG MUSCLE.

Richard Hahin and Donald T. Campbell, Dept. Physiology & Biophysics, University of Iowa, Iowa City, IA 52242

The vaseline gap technique was used to measure sodium channel gating currents in single bullfrog skeletal muscle fibers at normal (7.3) and low extracellular pH (6.0 and 5.0). External solutions contained (mM) TEA (110), Cs (5), Ca (2), HEPES or MES buffer (10), and TTX (4  $\mu\text{M}$ ); fiber ends were cut in CsF (113), NaF (5) and HEPES (10) (pH 7.2). Fibers were held at -150 mV to remove charge immobilization and permit the entire charge vs voltage (Q vs V) relation to be measured with depolarizing steps (range -135 to +45 mV).

In agreement with Neumcke, et al. (Biophys. J., 31:325) low pH reversibly slows gating current time course. At test potentials between 0 and 30 mV, time constants for exponential fits to "on" gating currents increased  $39 \pm 12\%$  (mean  $\pm$  SD,  $n=6$ ) at pH 6 and  $123 \pm 24\%$  ( $n=9$ ) at pH 5. In contrast to their results, peak charge was unchanged ( $\pm 5\%$ ) at pH 6 and was reduced  $20 \pm 1\%$  at pH 5. Low pH reversibly shifted the Q vs V relationship in the depolarizing direction by  $4 \pm 2$  (pH 6) and  $23 \pm 1$  (pH 5) mV. This shift in Q vs V is identical to shifts in Na current activation measured in muscle (Campbell and Hille, *J. Gen Physiol.*, 67:309) attributed to altered surface potential. The slowing of gating current time course is too great to be explained by a similar voltage shift. Supported by NS 15400 and MDA.

**T-PM-Po109** EFFECT OF INTERNAL  $\text{Cs}^+$  ON THE EARLY AND LATE CONDUCTANCE IN SQUID AXON: ARE "Na $^+$

CHANNEL" AND "K $^+$  CHANNEL" COUPLED? D.C. Chang, Department of Physiology, Baylor College of Medicine, Houston, TX, 77030 and Department of Physics, Rice University, Houston, TX 77001.

Perfusion of  $\text{Cs}^+$  inside the squid axon can result in suppression of the late current (or "K $^+$  current"). The action of  $\text{Cs}^+$  is time and voltage dependent and varies with the concentration of  $\text{Cs}^+$ . For an axon perfused with 400 mM K $^+$  and 100 mM  $\text{Cs}^+$ , the  $\text{Cs}^+$  begins to suppress the late current when the membrane potential (V) reaches approximately 40 mV. At 5 °C, the effect begins about 2 msec after the axon is depolarized and saturates at  $t = 6$  msec. In addition to affecting the late conductance, internal  $\text{Cs}^+$  also partly removes the inactivation of the early conductance (or "Na $^+$  conductance"). This effect also is time, voltage, and concentration dependent. To investigate whether the effects of  $\text{Cs}^+$  on early conductance and late conductance are related, we examined their dependence on each of the variables that could be controlled experimentally: time, cellular potential, and  $\text{Cs}^+$  concentration. We found that the  $t$ , V, and concentration dependence of the effects of  $\text{Cs}^+$  on early conductance and late conductance are similar. Whenever the late current is suppressed by  $\text{Cs}^+$ , a component of unactivated early current is created. This finding suggests that the gating mechanisms of the early conductance pathway ("Na $^+$  channel") and the late conductance pathway ("K $^+$  channel") may be coupled. (Work supported by ONR contract N0004-76-C-0100 p-B).

**T-PM-Po110 THE PROPERTIES OF K CHANNEL INACTIVATION IN PERFUSED SQUID GIANT AXONS.**

Lee D. Chabala (Intr. by H. Lester) Dept. of Physiology, Univ. of Rochester, Rochester, NY 14642.

The steady-state and kinetic properties of K channel inactivation were studied in the perfused squid giant axon. A depolarized holding potential of -49 mV was used to shift the steady-state occupancy of the K channel into inactive states. The kinetics of inactivation were monitored by applying a 7.5-msec test pulse followed by a long (usually 1 or 2 sec) conditioning pulse. This cyclic pattern was repeated until a new steady-state level of inactivation associated with the applied voltage had been reached. Both recovery from and development of inactivation were described by the sum of two voltage-dependent exponential terms (each with a  $Q_{10}$  of about 3). The steady-state inactivation curve is incomplete in the depolarizing region. At a standard holding potential of -69 mV, only about 5% of the K channels are inactivated. At the depolarized holding potential of -49 mV, more than 50% of the K channels are inactivated, and an apparent plateau corresponding to about 75% inactivation is reached near -29 mV. Instantaneous I-Vs and experiments in elevated external potassium ruled out changes in the driving force as an alternative explanation for the results. Most of the kinetic observations could be described by two distinct versions of a simple three-state kinetic model with exponential rate constants. If the K channels form a homogeneous population of identical and independent channels, then the asymmetry in the steady-state inactivation curve suggests that all three states are open but that the final open state has a low relative conductance assigned to it. In the second version, two populations of K channels are assumed, those with and those without an inactivation mechanism. In this latter instance, the asymmetry in the steady-state inactivation curve suggests that only the first two states are open.

**T-PM-Po111 SODIUM CHANNEL COMPARISONS BASED UPON RATES OF UNBINDING OF ANESTHETIC DRUGS**

Kenneth R. Courtney, Palo Alto Medical Foundation, Palo Alto, CA

Sodium channel block by many drugs can be modulated by rapidly using the channel. After block of the channel is changed by rapid trains of hyperpolarizing prepulses, depolarizing pulses or action potentials then channel block relaxes back to the resting or basal block level (b) with time constants (T) that are very drug-structure dependent. Sodium channels in myelinated nerve and skeletal muscle (of bullfrog) and cardiac muscle (papillary muscle of guinea pig) have been compared here regarding the rates of drug unbinding [ $\ell = (1-b)/T$ ] after these rapid periods of use. Surprisingly, cardiac channels resemble those of skeletal muscle in that considerations of both molecular weight (mw) and lipid distribution coefficient (log Q) were needed to fit these unbinding rates for each drug. However, drug size alone adequately fit the myelinated nerve unbinding rates.

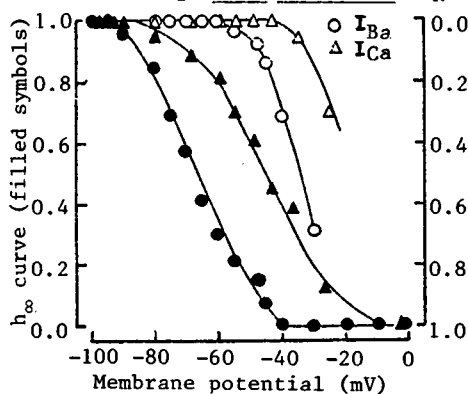
Preparation	Number of Drugs	Range of $\ell$ 's	Regression Fit Using	
			mw	mw + log Q
Frog myelinated nerve	16	0.02-.5 sec <sup>-1</sup>	R=0.73	R=0.74
Frog skeletal muscle	8	0.03-.4	0.37 →	0.76
Guinea pig papillary muscle	8	.15-5	0.72 →	0.97

Small log Q values may not limit drug escape from nerve channels (as they appear to do in muscle) because of the large, myelin lipid pool. It is also possible that muscle channels may differ from those in nerve. (Supported by NIH grants HL24156 and NS15914.)

**T-PM-Po112 CURRENT-INDEPENDENT INACTIVATION OF THE CALCIUM CHANNEL IN FROG SKELETAL MUSCLE.**

G. Cota, L. Nicola Siri and E. Stefani. Department of Physiology and Biophysics, Centro de Investigación del IPN, A-P 14-740, México, D.F. 07000.

The three microelectrode voltage clamp near the fibre end was used on cutaneous pectoris muscle fibres of large *Rana moctezuma*.  $I_K$  were blocked by incubating the muscles overnight at 4°C in (mM): TEA-Cl 60, CsCl 60 and  $CaCl_2$  1.8, under continuous agitation.  $I_{Ca}$  or  $I_{Ba}$  were recorded in (mM): TEA- $CH_3SO_3$  120,  $Ca(CH_3SO_3)_2$  10 or  $Ba(CH_3SO_3)_2$  10 and sucrose 350. Two pulse inactivation experiments at 22-23°C were performed. The figure shows that the current ( $I_{Ca}$  or  $I_{Ba}$ ) during the test pulse (about to 0 mV) was reduced to about 50% without any detectable inward current during the conditioning prepulse (7 sec). The steady-state inactivation curves were fitted to  $h_\infty = \{1 + \exp[(E_m - E)/k]\}^{-1}$  with  $E = -44$  mV and  $k = 9.1$  mV for  $I_{Ca}$  and  $E = -64$  mV and  $k = 5.2$  mV for  $I_{Ba}$  (six fibres). The decay of  $I_{Ca}$  and  $I_{Ba}$  followed a single exponential which had similar values in control and inactivated currents. The rate of decay measured at the peak of the current-voltage relation ( $\tau_{ca}$  to 0 mV for  $I_{Ca}$  and  $\tau_{ba}$  to -20 mV for  $I_{Ba}$ ) had the same value for both  $I_{Ca}$  and  $I_{Ba}$ . In conclusion, in this channel, inactivation is mainly voltage-dependent and Ca entry is not indispensable.



**T-PM-Po113 VOLTAGE CLAMP ANALYSIS OF A SPERM-GATED ION CHANNEL IN STARFISH EGGS.**

J. B. Lansman. Dept. of Physiology, School of Medicine, Univ. of California, Los Angeles, CA.

Membrane currents activated by sperm during fertilization in mature eggs of the starfish, *Mediaster aequalis*, were studied with the voltage clamp technique. In this egg, sperm trigger a depolarizing fertilization potential which reaches a peak of +10 mV in 10-15 min. and lasts as long as 30 min. before repolarizing. Under voltage clamp at the resting potential (-60 to -70 mV), this is seen as a slow inward current which follows a time course similar to the potential change. Voltage jumps were applied to the membrane at various times during the fertilization current. The instantaneous conductance reached a maximum at the peak of the fertilization current and then decreased. The time course of the sperm-activated conductance satisfactorily accounted for the time-dependent ionic current. The instantaneous I-V relations were linear and the reversal potential for current through the sperm-gated channel was +8 to +14 mV in normal seawater. Voltage steps to potentials more positive than -45 mV activate a transient Ca current. During fertilization, the Ca current relaxed to a steady-state value which was identical to the instantaneous value of the current through the sperm-gated channel. No voltage-dependent relaxations of the sperm-activated current were detected over the potential range -70 to +10 mV. Application of a current subtraction procedure indicates that fertilization does not alter the I-V properties of the egg membrane Ca current and that the sperm-gated channels act as a parallel pathway for current flow. Sperm-gated channels may, thus, resemble receptor-gated ion channels in being relatively non-selective and voltage-insensitive. (Supported by USPHS GM7191, MH15345, and NS09012)

**T-PM-Po114 A MODEL OF THE SODIUM CHANNELS IN NERVE AXONS. K.C. Ho and W.X. Yang, Nankai University, Tianjin, The People's Republic of China (Intr. by L. D. Peachey)**

The protein molecules embedded in nerve axon membranes carry out the function of sodium channels. Along the direction across the membrane, the parts of a protein molecule that are close to the fatty acid chains form a number of nearly parallel  $\alpha$ -helices. The polarized side chains extend to fill the space between the helices. Two kinds of stable conformation may be formed. In conformation I, hydrogen or ionic bonds are formed by pairs of dipoles or charges through the action of the membrane potential. In conformation II, the side chains remain at the lowest energy state which is decided only by structural factors. They cause the channel to appear in the closed or open state respectively. The probability for a side chain being in conformation I or II is determined by the Boltzmann law. The sodium ions pass through the energy barrier by way of jumping diffusion. In accord with the polarizing properties of a dielectric under the action of an electric field, some expressions are derived for the kinetic properties of a "gating" current and sodium conductance. These are functions of membrane potential and time. Numerical calculations using these expressions may fit the various experimental results fairly well.

**T-PM-Po115 INTERACTIVE EFFECTS OF CYTOPLASMIC ACIDIFICATION AND VOLTAGE ON CONDUCTANCE OF GAP**

JUNCTIONS BETWEEN SQUID BLASTOMERES, M.V.L. Bennett, A.L. Harris, D.C. Spray, R.D. Ginzberg\* and E.A. Morales\*, Dept. Neuroscience, Albert Einstein Col. of Med., Bronx, N.Y. 10461.

Cleavage stage blastomeres of *Loligo* are electrotonically and dye coupled and joined by gap junctions. Cell pairs prepared by dissection were studied by current or voltage clamp. Acidifying the cell interior by bathing in weak acids rapidly and reversibly decreases junctional conductance ( $g_j$ ) and uncouples the cells. As  $g_j$  nears or reaches zero, large polarizations of one cell can cause a slow somewhat noisy approximately exponential increase in  $g_j$  to a new steady state value up to about 10% of the pre-acid value. The relation of steady state  $g_j$  to transjunctional voltage ( $V_j$ ) when one cell is polarized is upwardly concave with no indication of saturation below 60mV.  $\tau$ 's of  $g_j$  increase, of the order of 1 sec, are shorter for larger  $V_j$ 's;  $\tau$ 's of exponential post-pulse decrease in  $g_j$  to its prepulse value are variable but may be as long as 5 sec. Increase in  $g_j$  is often asymmetric, in that it is produced by hyperpolarizing one cell but not the other. The increase is not dependent only on  $V_j$ , because hyperpolarizing one cell can differ from depolarizing the other, and hyperpolarizing both cells simultaneously may also produce a small increase. Further cytoplasmic acidification causes the voltage dependence of  $g_j$  to disappear, and on rinsing with normal sea water, voltage dependence returns before  $g_j$  begins to recover. These data suggest that over a range of low  $pH_i$ , closure of junctional channels involves a conformational change producing dipole moment changes acted on by both the transjunctional field and the field between inside and outside of the cells. Disappearance of voltage dependence at still lower  $pH_i$  suggests decreased dipole moment changes or stabilization of channels in the closed conformation. Voltage dependence has not been studied at normal  $pH_i$  because of high values of  $g_j$ .

**T-PM-Po116** THE EFFECT OF MONOVALENT CATIONS ON THE CONFORMATION OF GRAMICIDIN A IN ORGANIC SOLVENTS.

M.R. Kimball and B.A. Wallace, Dept. of Biochemistry, Columbia University, NY NY 10032.

The conformation of gramicidin A undergoes a considerable change in solvents such as methanol, ethanol or dioxane when monovalent cations are introduced into the system. The exact nature of this change is currently under investigation by circular dichroism spectroscopy and X-ray crystallography. In no instance are the structures observed similar to the membrane-bound gramicidin structure, which is insensitive to the presence of cations (B.A. Wallace, W.R. Veatch and E.R. Blout, *Biochemistry*, **20**, (1981) 5654-5760). The experimental data are consistent with the hypothesis that cation-binding stabilizes a helical conformation of the opposite hand from that which predominates in systems without cations. Furthermore, the pitch of the helix and consequent channel dimensions depend on cation size. Approximate differences in pitch, as well as binding constants, have been derived from the spectroscopic data. Since the Gramicidin/Cs<sup>+</sup> and Gramicidin/Li<sup>+</sup> complexes show the greatest differences in geometry, these complexes have been crystallized and are now being analyzed by X-ray diffraction methods. The results are consistent with those obtained from crystals of gramicidin complexed with the other alkali metal cations as well as with Tl<sup>+</sup>. The crystallographic data are expected to provide detailed information concerning the dependence of helix geometry on cation size.

Supported by NSF grant PCM 80-20063.

**T-PM-Po117** INDUCTION OF SLOW ACTION POTENTIALS BY PRESSURE INJECTION OF CYCLIC AMP INTO HEART CELLS. T. Li and N. Sperelakis. Physiology Dept., University of Virginia, Charlottesville, VA 22908.

There is strong evidence that the functioning of the slow channels is dependent on the intracellular cyclic AMP level. Vogel and Sperelakis (*J. Mol. Cell. Cardiol.* **13**:51-64, 1981) demonstrated that iontophoretic injection of cyclic AMP induced and potentiated slow action potentials (APs) in dog Purkinje fibers and guinea pig papillary muscle cells. In the present study, cyclic nucleotides in various combinations were pressure injected into guinea-pig ventricular papillary muscle superfused with Tyrode solution (37°C). The fast Na channels were inactivated by partial depolarization to about -40 mV in 21 mM [K]<sub>o</sub>. Stimulations at 60/min and just sub-threshold were used. Induction of slow-rising APs indicated an increase in slow conductance and slow inward current (I<sub>si</sub>). Microelectrodes filled with 1 M Na-cyclic AMP (beveled from >30 MΩ to 10-15 MΩ to facilitate injections) were used for both monitoring membrane potentials and intracellular injections with pressures of 40 to 80 psi. Slow APs, with V<sub>max</sub> of 4-8 V/sec and duration of 40-75 msec, were usually induced within 30 sec after starting the injection (continuous) in 11 out of 12 cells tested. They disappeared within 0.5 - 2 min after injection was stopped. Na-AMP injection had no effect. Injection of cyclic GMP (with microelectrodes filled with 0.1 - 0.2 M Na-cyclic GMP) into cells exposed to 10<sup>-6</sup> M isoproterenol to induce large slow APs (V<sub>max</sub> of ~30 V/s, duration of 150-200 msec) gave variable results. Some cells tested showed a depression of AP plateau amplitude, whereas the other cells showed no effect. The present results provide further support that a relationship between cyclic AMP and I<sub>si</sub> exists. These findings are consistent with the hypothesis that phosphorylation of the slow channel protein by a cyclic AMP-dependent protein kinase makes the slow channel available for voltage activation. (Supported by NIH grant HL-18711.)

**T-PM-Po118** KINETICS OF THE Ca<sup>2+</sup>-ACTIVATED K<sup>+</sup> CHANNEL IN CULTURED RAT MUSCLE. Barry S. Pallotta, Karl L. Magleby, and John N. Barrett\*, Dept. Physiology & Biophysics, University of Miami School of Medicine, Miami, FL 33101.

Using extracellular patch clamp techniques, we have studied the Ca<sup>2+</sup> and voltage sensitivity of Ca<sup>2+</sup>-activated K<sup>+</sup> channels in excised membrane patches. At +20 mV membrane potential, the relation between log[Ca<sup>2+</sup>] at the intracellular surface of the membrane patch versus % of time open was S-shaped; channels were open <1% of the time in 0.1 μM Ca<sup>2+</sup> and >90% of the time in 100 μM Ca<sup>2+</sup>. Channel activity was also sensitive to membrane polarization such that % of time open varied from <1% to ~80% in 1 μM Ca<sup>2+</sup> when the membrane potential was clamped from -50 to +50 mV. Channel activity was less sensitive to voltage at very low (0.01 μM) or high (100 μM) Ca<sup>2+</sup>. Once open, channel closing rates were also found to vary such that channel open times were prolonged by increasing [Ca<sup>2+</sup>]<sub>i</sub> and membrane depolarization. The effects of Ca<sup>2+</sup> and voltage were readily reversible.

When recording from patches in which only one channel could be activated, we observed that channel activity occurred in bursts of openings; histograms of all closed intervals were described by two exponentials. The slower component corresponded to the interburst interval, and the faster reflected the brief closed periods during the bursts. Interburst interval decreased from 2000 to 1.5 msec as [Ca<sup>2+</sup>]<sub>i</sub> was increased from 0.1 to 50 μM. Burst duration increased with increasing [Ca<sup>2+</sup>]<sub>i</sub>, suggesting that there is more than one Ca<sup>2+</sup> binding site which affects channel activity. Membrane depolarization also increased burst duration and decreased interburst interval. Supported by NIH grants NS 10277, NS 06081, NS 12207, and the Muscular Dystrophy Association.

**T-PM-Po119** CONTRAST BETWEEN OPEN AND CLOSED BLOCK OF SINGLE Na CHANNEL CURRENTS. F.N. QUANDT, J.Z. YEY, AND T. NARAHASHI. DEPT. OF PHARMACOL., NORTHWESTERN UNIV. MED. SCH., CHICAGO, IL 60611.

We have examined the effects of prototype open and closed Na channel blocking molecules on currents through single Na channels as measured with the "outside-out" patch-clamp technique (Hamill et. al., Pflugers Arch. 391:85, 1981) using N1E-115 neuroblastoma cells. Characteristics of the block of Na channels by tetrodotoxin (TTX) were consistent with closed channel block. TTX caused a dose-dependent reduction in the number of channels available to conduct in response to a series of depolarizations when applied externally to the excised patch of membrane. The apparent  $K_d$  was 2 nM. The channels remaining at lower concentrations of TTX have normal conductance and open times. In one typical experiment, the single channel current was  $1.47 \pm 0.37$  pA before and  $1.24 \pm 0.24$  pA after exposure to 20 nM TTX, whereas mean open time was 2.2 msec before and 2.1 msec after exposure (-40 mV, 9°C). In contrast, 9-aminoacridine (9-AA) alters the temporal properties of Na channel currents, consistent with a block of the open channel. Exposure of the patch of membrane to 5  $\mu$ M batrachotoxin causes long-lasting Na channel currents to appear spontaneously if the holding potential is reduced to potentials less negative than -80 mV. In one typical experiment, the mean open time of these modified currents was 52 msec (-65 mV, 8°C). Following the external application of 300  $\mu$ M 9-AA; short-duration, frequent interruptions to the zero current level were observed only following the opening of the Na channels. The mean duration of the interruptions was approximately 5 msec for this experiment and the mean period between interruptions was approximately 20 msec. Channel conductance was not affected by 9-AA. Supported by NIH grants NS 14144 and GM 24866.

**T-PM-Po120** CYTOPLASMIC STX BINDING SITES IN AMPHIBIAN MYOCARDIUM. L. Barr, D. Doyle\* and J. Tanaka\*\*. Department of Physiology and Biophysics, University of Illinois, Urbana, IL 61801.

Heretofore, STX has been found to bind with saturating kinetics quite specifically to the plasma membranes of excitable cells which utilize inward Na current to generate the upstroke of their action potentials. We have found high affinity STX binding sites in the cytosolic fractions of homogenates of myocardia from *Rana pipiens*, *Rana catesbeiana* and *Bufo marinus*. We found no such sites in the cytosolic fractions of homogenates of eel electroplax or myocardia from adult chicken or turtle. The amount of binding of  $^3$ H-STX per unit tissue was about 5 times greater in the cytosolic fraction of frog myocardia than in either the whole heart or the plasma membrane fractions. Sephacryl column chromatography gave a Stokes radius of about 52 Å for the cytoplasmic STX site. The appearance of the site in the cytosol was not decreased by the presence of EDTA, iodoacetate, PMSF, leupeptin, pepstatin or variation of ionic strength or changing the tactics to isolate sarcolemmal vesicles. Isoelectric focusing of the cytosolic STX binding site yielded several peaks, all between pH 6.7 and 7.6. The STX binding activities in these peaks was about 6 times greater than in the cytosol. When eel electroplax homogenates were incubated with frog myocardial homogenates the amounts of STX binding in the vesicular and cytosolic fractions was unchanged. On the basis of these data we formed the working hypothesis that the cytosolic sites came from the cytoplasm.

\* Presently at the Department of Physiology, University of Illinois: Medical Campus

\*\*Presently at the Department of Biochemistry, University of Pennsylvania

**T-PM-Po121** BINDING OF  $^3$ H-STX TO MYOCARDIAL SARCOLEMMMA FROM SEVERAL SPECIES. J. Tanaka\* and L. Barr, Department of Physiology and Biophysics, University of Illinois, Urbana, IL 61801.

Measurements of  $^3$ H-STX binding to partially purified myocardial sarcolemmal vesicles indicate that some myocardial sarcolemmae differ significantly in their STX affinities from those of the plasma membranes of skeletal muscles and nerves. Sarcolemmal preparations were isolated from homogenates by sucrose gradient centrifugation. Myocardial vesicles were pelleted from  $^3$ H-STX incubation media by centrifugation at 45 KXg for 30 minutes then rinsed quickly and counted. The dissociation constants and site densities were determined from the concentration dependent amount of  $^3$ H-STX bound, obtained by subtracting the amounts of the linear binding component in the presence of  $10^{-5}$  M unlabelled STX from the total amounts of  $^3$ H-STX bound. The sarcolemmae of amphibian myocardia (*Rana pipiens*, *Rana catesbeiana* and *Bufo marinus*) have a high affinity ( $K_D < 10^{-8}$  M) which is similar to skeletal muscle and nerve. However, adult chicken and turtle myocardia appeared to have only sites of much smaller affinity. The dissociation constant for chicken myocardial sarcolemma was  $1.75 \times 10^{-6}$  M and that for turtle myocardial sarcolemma was  $1.45 \times 10^{-6}$  M. The STX affinities of chicken and turtle preparations were measured by a self competition assay using increasing concentrations of unlabelled STX in the presence of a constant concentration of  $^3$ H-STX. A Hill plot was used to estimate the  $K_D$ s of the chicken and turtle myocardial sarcolemmae. We conclude that the Na channels of adult chicken and turtle myocardia differ in their affinities for STX by two orders of magnitude from those of amphibian myocardia and skeletal muscle and nerve in general.

\* Present address: Department of Biochemistry, University of Pennsylvania

**T-PM-Po122** THE EXPRESSION OF SODIUM CHANNELS IN DEVELOPING SKELETAL MUSCLE IN CULTURE. G. Strichartz, D. Bar-Sargi and J. Prives., Anesthesia Res. Labs., Harvard Medical School, Boston, MA. 02115 and Dept. of Anatomical Sci, HSC, SUNY Stony Brook, N.Y. 11794

During muscle cell fusion and development in culture, the appearance of receptors for  $^3H$ -STX(\*STX) and the  $^{22}Na$ -flux catalyzed by batrachotoxin (BTX-flux) have been followed. BTX-flux (at  $10^{-6}M$ ) is clearly present at 2d after cell plating, but \*STX binding (at  $4nM$ ) is not detectable until day 3. At day 7 BTX-flux has doubled while \*STX binding has grown  $\sim 8$ -fold. Only half of the BTX-flux is blocked by  $20nM$  TTX in 3d cells, whereas  $>90\%$  is blocked in 7d cells. These muscle cells express a TTX-resistant sodium channel at first; later only a normally TTX-sensitive channel is detectable. The appearance of receptors for STX(TTX) parallels closely the value of  $\dot{V}_{max}$ . After 24h. exposure of 3d cells to an inhibitor of protein synthesis, cycloheximide (CHX), both BTX-flux and \*STX binding are reduced, by 40% and 70%, respectively, both activities recover partially upon removal of CHX. In contrast, neither flux nor binding is depressed by more than  $\sim 10\%$  in 7d cells exposed to CHX. The relationship between TTX(STX)-sensitivity, channel subunits, and the voltage-dependence of sodium channels will be described further.

1. Spector, I, & Prives, J.M. *Proc. Natl. Acad. Sci. USA.* 74: 5166 (1977)

Supported by USPHS grant NS12828 and MDA research grant (to GS), and an MDA research grant to J.P.

**T-PM-Po123** VERATRIDINE MODIFICATION OF THE NERVE MEMBRANE SODIUM CHANNEL. Virginia M. Scruggs and Toshio Narahashi, Dept. of Pharmacology, Northwestern Univ. Med. Sch., Chicago, IL 60611.

The mechanisms underlying modification of Na channel kinetics by veratridine were studied using voltage-clamped, squid giant axons perfused externally with K-free, low Na sea water and internally with K-free, 50 mM Na solution at  $12^\circ C$ . When treated internally with  $25 \mu M$  veratridine, depolarization to 0 mV produced the transient Na current ( $I_{Na}$ ) followed by a slow, tetrodotoxin-sensitive  $I_{Na}$  with a half-time to maximum of about 165 ms. The transient current underwent little kinetic change except for a 5-10% decrease in peak amplitude. The slow tail current following repolarization was also sensitive to tetrodotoxin. Its decay could be expressed as two exponential components with time constants of about 90 ms and 470 ms. The rise of the slow  $I_{Na}$  contained two major components in its development with time constants of about 105 ms and 395 ms. The slow process accounted for about 75% of the total. When Na inactivation was removed internally with pronase, the slow  $I_{Na}$  decay rate was unchanged whereas its formation was greatly accelerated and potentiated. The time to reach half maximum was decreased to 10 ms—a 15-fold change relative to nonpronased axons. The rise-time had two major components with approximately 15 ms and 125 ms time constants and the most rapid component contributed about 85% to the total slow  $I_{Na}$ . The multicomponent development and decay of the slow  $I_{Na}$  suggest that more than one pathway or process is involved in formation of and recovery from the veratridine-modified Na channel. The above findings are consistent with a hypothesis in which both open and closed states of the Na channel are precursors to the veratridine-modified open state. Supported by NIH grant NS 14144.

**T-PM-Po124** LYOTROPIC ANIONS SHIFT THE VOLTAGE DEPENDENCE OF GATING IN Na CHANNELS OF MUSCLE. Jorge Sanchez, John A. Dani, and Bertil Hille. Dept. Physiology and Biophysics, Univ. of Washington, Seattle, Wash.

Lyotropic anions influence many properties of excitable cells. They reduce the threshold of K contractures (Hodgkin & Horowicz, 1960) and of delayed rectifier K channels (Kao & Stanfield, 1968) of frog skeletal. Using the Hille-Campbell voltage clamp technique to measure peak Na currents, we found that anions shift the voltage dependence of Na channel activation and inactivation as well. The ends of single frog muscle fibers were cut in isotonic CsF, and the external reference solution was  $Cl^-$  Ringer. In the test solutions the  $Cl^-$  was partially or completely replaced by another anion. Lyotropic anions shifted activation and inactivation by as much as -17 mV after correcting for junction potentials. The shifts were generally negative and larger for inactivation than activation. The sequence of effectiveness was  $CH_3SO_3^- < Cl^- < CH_3COO^- < Br^- < NO_3^- < SO_4^{2-} < SCN^- < ClO_4^-$ . The steepness of the activation or inactivation curves and the maximum sodium permeability differed less than 22% between the test and reference solutions. The anion effects are similar to those seen when the external  $Ca^{++}$  activity is lowered. However, spectrophotometric experiments with the metallochromic  $Ca^{++}$  indicator murexide showed that only  $SO_4^{2-}$  decreases  $Ca^{++}$  activity. Further muscle experiments indicated that calcium and anion effects are simply additive at the concentrations used. The lyotropic series is observed in many studies of interfaces of water with macromolecules or hydrophobic phases. Hodgkin and Horowicz (1960) proposed that adsorption of these anions at the membrane surface alters the immediate electric field and influences gating. (Supported by NIH grant NS08174)



**T-PM-Po125 LYOTROPIC ANIONS AFFECT A Ca-SELECTIVE ELECTRODE.** John A. Dani, Jorge Sanchez, Bertil Hille. Dept. of Physiology and Biophysics, Univ. of Washington, Seattle, Wash.

Studying the effect of anions on the voltage dependence of Na channel gating in muscle, we discovered that some anions interact with a Ca-sensitive, ion-selective electrode. Measurements were made with an Orion Research Inc. 93-20 Ca electrode with a 93-20-01 Ca-sensing module referenced against a Corning calomel-saturated KCl, fiber junction electrode. The solutions were well stirred and measurements with  $\text{Ca}^{2+}$  standards were repeatedly made to guard against drift in the response or possible irreversible effects due to the anions. Relative to the expected Nernstian response of the electrode to  $\text{Ca}^{2+}$  in  $\text{Cl}^-$  solutions, other anions generally caused negative shifts of the electrode output (in some cases greater than -100 mV), accompanied by a reversible decrease or even elimination of the  $\text{Ca}^{2+}$  sensitivity of the electrode. The sequence of effectiveness was:  $\text{SO}_4^{2-} < \text{CH}_3\text{SO}_3^- < \text{Cl}^- < \text{Br}^- < \text{CH}_3\text{COO}^- < \text{SO}_3^- < \text{NO}_3^- < \text{SCN}^- < \text{ClO}_4^-$ . The possibility that these anions act by binding free  $\text{Ca}^{2+}$  ions was ruled out by spectrophotometric measurements of  $\text{Ca}^{2+}$  activity with the metallochromic  $\text{Ca}^{2+}$  indicator murexide. Only  $\text{SO}_4^{2-}$  binds  $\text{Ca}^{2+}$ . Furthermore potential shifts could be obtained even in the absence of  $\text{Ca}^{2+}$ . Other tests showed that the potentials did not arise at the reference electrode. Qualitatively the liquid membrane electrode seems to respond both to  $\text{Ca}^{2+}$  ions and to lyotropic anions. The results could be fitted quantitatively by assuming that the electrode membrane contains a saturable  $\text{Ca}^{2+}$  carrier and is also permeable to the anions. Thus in addition to their well-known actions on macromolecules and interfaces, lyotropic anions may quite generally affect electrodes with hydrophobic liquid membranes. (Supported by NIH grant NS 08174)

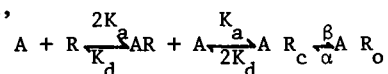
**T-PM-Po126 EXPECTED GATING CURRENT FROM THE AGGREGATION GATING SITE.**

Gilbert Baumann, Department of Physiology, Duke University Medical Center, Durham, NC 27710, and George S. Easton, Department of Statistics, Princeton University, Princeton, NJ 08540.

Expected gating currents are derived analytically from a continuous, time-homogenous Markov process formulation of the random behavior of a single hypothetical aggregation gating site consisting of four subunit molecules. The concept of aggregation gating involves a voltage-dependent reversible conformational change followed by a voltage-independent reversible aggregation process. The model can account for the phenomenon of charge immobilization in asymmetry current data of the voltage-clamped sodium conductance system. Furthermore, the model predicts gating currents without a rising phase. An artifactual rising phase is obtained, however, if the model is subjected to conventional symmetrical pulse protocols for measuring asymmetry currents in the axon. Novel experimental pulse protocols for measuring asymmetry currents in the axon are proposed that eliminate the artifactual rising phase if applied to the aggregation model. A simplified aggregation model that can account for the basic kinetic behavior of the potassium conductance system and one that can account for the basic kinetic behavior of the sodium conductance system are presented. These simplified schemes resemble empirical models that have been published by others. (Supported by NSF grant PCM78-02802 and NIH grant GM27260).

**T-PM-Po127 AGONIST AND CHANNEL KINETICS OF THE NICOTINIC ACETYLCHOLINE RECEPTOR.** D. Nelson\* & F. Sachs, Dept. of Biophysical Sciences, SUNY/Buffalo, Buffalo, NY 14214. \*Present address: Dept. of Physiology, Rush Medical Center, Chicago, Ill.

We have measured the kinetics of single nicotinic channels in tissue cultured chick skeletal muscle. The data shows bursts of activity which are interpreted as repeated openings of a single channel. The length of the bursts increases with hyperpolarization, showing a voltage dependence of about 35 mV/e fold change for acetylcholine (ACh). Interpreted according to a four state sequential model,



the most profound effect of potential is to affect the rate of dissociation, rather than channel opening or closing rates. Typical rate constants for ACh at -100 mV, 10°C are  $\alpha = 45/\text{sec}$ ,  $\beta = 1000/\text{sec}$ ,  $k_d = 80/\text{sec}$ ,  $k_c = 3 \times 10^7/\text{M}/\text{sec}$ , half saturation concentration,  $C_{0.5} = 1 \mu\text{M}$ . For carbachol  $\alpha = 20/\text{sec}$ ,  $\beta = 250/\text{sec}$ ,  $k_d = 300/\text{sec}$ ,  $k_c = 10^5/\text{sec}$  and  $C_{0.5} = 0.5 \text{ mM}$ .

The number of channels in the patch, a number which is necessary to calculate  $K_a$ , was taken as the highest order multiple observed in the record. This is a lower limit, and places an upper limit on  $K_a$  and a lower limit on  $C_{0.5}$ .

**T-PM-Po128** SINGLE CHANNEL CURRENTS FROM HELA CANCER CELLS. Rémy Sauvé and Guy Roy, Department of Physics, University of Montreal, Montreal, CANADA

We used the extracellular patch clamp technique introduced by Neher et al. in order to investigate the presence of ionic channels in Hela cell, a well-known culture cell type obtained from an epidermoid carcinoma of the cervix. Gigohm-seal could be established without enzymatic treatment of the cell surface. Under Gigohm-seal condition, discrete current jumps could be observed with patch electrode containing KCl. The presence of potassium in the electrode seemed to be critical, since experiments carried out with NaCl failed to show equivalent single channel events. Single channel I/V curves were measured with patch electrode containing KCl in various concentrations. At 0.15M KCl, a concentration which eliminates the K gradient between the patch pipette and the cell interior, an important rectification effect, characterized by a large inward and a small outward current was observed. Within the inward current voltage range (0- -60mV) the I/V curves were almost linear corresponding to a single channel conductance of  $24 \pm 2$  pS. Experiments at a higher KCl concentration (0.3) did not result in a significant increase of the single channel conductance. The channel mean life time in 0.15 KCl was estimated at 1 sec. at room temperature. This slow process was coupled to a fast on-and-off mechanism occurring during channel opening. The time distribution of the slow opening process could be well fitted by a single exponential, meaning that these single channel events behave in a statistically independent manner. The ionic specificity and the effect of divalent cations will also be discussed.

(1) Neher, E., Sakmann, B. and Steinbach, J.H., 1978. PFLUG. ARCH. 375; 219-228.

**T-PM-Po129 SINGLE CHANNEL CONDUCTANCES FORMED BY DIPHTHERIA TOXIN FRAGMENTS IN PLANAR BILAYERS.**

Stanley Misler, Bruce L. Kagan and Alan Finkelstein. (Intr. by B. Wittenberg) Depts. of Physiology & Biophysics and Medicine (Nephrology), Albert Einstein College of Medicine, Bronx, NY.

CRM45 and B45 are fragments of diphtheria toxin which induce moderately voltage-dependent conductances in bilayer membranes. CRM45 consists of the entire A fragment, shown to be enzymatically active intracellularly and B45. B45 is a large portion of the B fragment postulated to serve as the channel through which the A fragment enters the cytoplasm. The conductance changes induced by CRM45 and B45 are due to cation selective single channels which have several interesting properties. (1) B45 and CRM45 single channel conductances ( $g_s$ ) are ohmic over a wide range of imposed clamping potentials ( $V_m$ ) from -140 to +140mV (cis) and increase with increases in either the salt concentration or pH. Typically, for B45 or CRM45,  $g_s$  changes from 5-7 pS in symmetric solutions of 0.1M KCl and pH 4.7; to 22-24 pS in symmetric 1M KCl, pH 4.7; to 5 pS in 1M KCl solutions where the cis to trans pH gradient is 5.5 to 7.4. (2) The rates of single channel opening ( $r_o$ ) and closing ( $r_c$ ) of both fragments show similar characteristic dependencies on  $V_m$  and pH. In symmetric pH 4.7 or 5.5, channels rarely open at 0mV.  $r_o > r_c$  at + $V_m$  (20-140mV) and  $r_o(V_m)$  increases more steeply than  $r_c(V_m)$ , whereas at - $V_m$ ,  $r_c > r_o$  with  $r_c(V_m)$  increasing more steeply than  $r_o(V_m)$ . (3) In the presence of a pH gradient (e.g. cis pH 4.7, trans pH 7.0), B45 and CRM45 channels are open at 0mV and at + $V_m \geq 70$ mV,  $r_c \geq r_o$ . These data suggest that (a) the presence of the A fragment does not detectably alter channel conductance and (b) the decay of macroscopic conductance at + $V_m > 70$ mV in the presence of a pH gradient may result from faster channel closing rates under these conditions.

**T-PM-Po130 SLOW INWARD Ca CURRENT IN FROG HEART: VOLTAGE-DEPENDENT OR Ca-MEDIATED INACTIVATION?** R. Fischmeister and M. Horackova, Dalhousie University, Halifax, N.S., Canada.

It has been recently suggested that Ca currents in various preparations, including cardiac muscle, might be inactivated by increase in  $[Ca]_i$ . To test this hypothesis, we have used a computer simulation of the action potential (AP) in frog heart to calculate the corresponding slow inward Ca current ( $I_{si}$ ) by using either a Hodgkin-Huxley (H-H) model of voltage-dependent inactivation or a model of Ca-mediated inactivation. According to the H-H model, the time course of  $I_{si}$  (with a time constant of inactivation,  $\tau_f$ , of 55 msec at -10mV) was biphasic; after a transient increase followed by a decrease to zero,  $I_{si}$  partially reactivated (at the beginning of the repolarization phase) and then fully deactivated. The reactivation phase of  $I_{si}$  developed whatever the relationship of  $\tau_f$  vs. membrane potential ( $E_m$ ). Such a variation of  $I_{si}$  should result in a biphasic curve of tension; however, there is to date no such experimental evidence. The simple model of Ca-mediated inactivation was based on a reversible  $Ca_i$  binding, forming functional groups which regulate Ca conductance. Calculated from the AP,  $I_{si}$  first decreased rapidly to  $\approx 25\%$  of its maximal value and then remained quasi-constant during the AP plateau; a complete deactivation of  $I_{si}$  occurred at repolarization. Using voltage-clamp simulation, this model gave an apparent "steady-state" inactivation which is a U-shaped function of  $E_m$ . Although this behaviour remains to be supported by further experimental data, our results indicate that the Ca-mediated process of  $I_{si}$  inactivation represents more realistically the behaviour of frog cardiac preparation than the voltage-dependent model.

(Supported by grants from the Nova Scotia Heart Foundation and from MRC of Canada, MT-4128.)

**T-PM-Po131 ANTIBODIES DIRECTED AGAINST THE TETRODOTOXIN-BINDING COMPONENT OF THE VOLTAGE-SENSITIVE SODIUM CHANNEL.** S.R. Levinson, J.A. Miller, Dept. Physiology, U. Colorado Med. Cntr., Denver, CO 80262, & M. Ellisman, Dept. Neurosciences, U. Calif. @San Diego, La Jolla, CA 92093.

Heterologous antisera and monoclonal antibodies have been raised against the tetrodotoxin-binding component (TTXR) from the electroplax of *E. electrophorus*. To assess the titer and specificity of these antibodies, a highly sensitive radioimmunoassay has been developed. This assay uses I-125 labelled TTXR as antigen, and is capable of detecting as little as 5 femto-moles of either TTXR-specific antibody or TTXR.

We have raised rabbit antisera to highly purified TTXRs and have used it to demonstrate sodium channels in various tissues of *E. electrophorus* using immunocytochemical techniques. We have also established two hybridoma cell lines which are producing monoclonal antibodies to TTXRs. These cell lines have been propagated as ascites tumors in mice, thus producing milligram quantities of the monoclonal antibodies for other studies.

When used in simple immunoaffinity procedures, these monoclonal antibodies can selectively isolate TTXRs from a partially-purified extract of electroplax membranes. SDS-PAGE analysis of the immunopurified material shows only a single polypeptide of  $M_r$  approx. 260,000 daltons. This finding lends support to the idea that, in the electric eel, the TTXR and possibly the entire sodium channel apparatus is comprised of a single species of polypeptide.

**T-PM-Po132** RECURRENT SODIUM ACTION POTENTIALS IN FROG OOCYTES. L.C.Schlichter( Intr. by R.T.Kado). Botany Dep't., Univ. of Toronto, Toronto, Ontario, Canada M5S 1A1

Spontaneous, recurrent Na action potentials have been observed in maturing frog oocytes (*R. pipiens*) during metaphase of the first meiotic division. Initially the spikes last 15 to 30s, the threshold for firing is -10 to 0 mV and for closing is +25 to 35 mV. Ion substitutions show that the peak amplitude responds in a Nernstian manner to changes in external Na activity and that inactivation depends on  $\text{Cl}^-$  influx. As maturation proceeds  $E_{\text{Na}}$  shifts from about +62 mV to +30 mV at metaphase II. This corresponds to an increase in internal sodium activity from 6mM to 22mM and is in excellent agreement with results obtained with Na-selective microelectrodes.

During maturation gCl decreases and the Cl-dependent inactivation disappears. At this time the spikes are no longer spontaneous but can be elicited in an all-or-none manner by injected current. The regenerative channels can then be closed during a pulse of hyperpolarizing current. Because the resting gNa is high at this stage they reopen when the current is turned off. External Ca or Co at 5mM closes the Na channels in a reversible manner and inhibits maturation. Similar results have been obtained with metaphase II oocytes of *R. clamitans*.

**T-PM-Po133** A SYMMETRIC MODEL FOR THE JOINT EFFECTS OF SCORPION TOXIN AND AN ALKALOID NEUROTOXIN. Gerald Ehrenstein, Li-Yen Mae Huang, and Nava Moran, NINCDS, NIH, Bethesda, MD 20205.

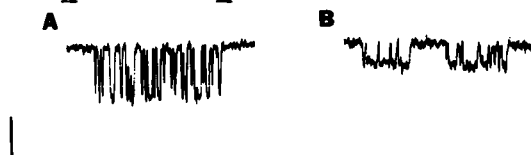
In order to explain the increases in sodium conductance caused by mixtures of scorpion toxin and an alkaloid neurotoxin (such as batrachotoxin or veratridine), we propose a model that treats the two components symmetrically. In this model, each toxin has a higher affinity for the activated sodium channel than for the resting sodium channel. Also, the only channels that have steady state conductance are activated channels bound to an alkaloid neurotoxin, to scorpion toxin, or to both.

This symmetric model fits the available data on increases in sodium conductance in the presence of the toxins. It also offers the following advantages:

- 1) It assigns a fixed equilibrium constant to each transition between a resting state and an activated state.
- 2) It provides a rationale for the experimental observation that either toxin alone can increase the sodium conductance.
- 3) It provides a rationale for the experimentally observed differences in slow inactivation between batrachotoxin-bound channels and scorpion-toxin-bound channels.
- 4) It is consistent with the relatively small influence of batrachotoxin on scorpion toxin binding.

**T-PM-Po134** SINGLE ACETYLCHOLINE CHANNEL BLOCK IN ELEVATED SODIUM AND LITHIUM. G.A. Redmann, R.B. Clark and P.R. Adams. Dept. of Physiology and Biophysics, UTMB, Galveston, TX. 77550

Acetylcholine channel currents in cultured BC3H1 myocytes were examined in intact cells and ripped-off membrane patches with the gigohm seal patch clamp technique. Currents were recorded via a pipette containing 100-400 nM acetylcholine and saline, which consisted of either 150 or 325 mM of either NaCl or LiCl, 5.6 mM KCl, 1.8 mM  $\text{CaCl}_2$ , 1.0 mM  $\text{MgCl}_2$ , 10 mM glucose and 10 mM Na-HEPES, at pH 7.3. Bath solutions were 150 mM, less the agonist. The I-V relation for both intact and ripped-off patches in 150 mM NaCl over a +150 to -150 mV range was linear, with a single channel conductance, g of  $34 \pm 2.6$  (S.D.) pS. The I-V for 150 mM LiCl was linear in symmetrical solutions with excised patches, g being  $17 \pm 2$  pS. Mean channel open time  $t_o$ , at 50 mV negative to rest and in 150 mM NaCl was  $20 \pm 23$  (S.D.) ms,  $t_o$  in 325 mM NaCl was 76 ms, and for 150 mM LiCl was  $38 \pm 39$  ms. Channel block by the local anesthetic QX-222 was analyzed to fit a 3-state sequential block model. Mean open times were inversely related to QX-222 concentration over the range 5-50  $\mu\text{M}$ , occurred in bursts (mean blocked time  $t_b$ ), and were voltage-dependent. Values for  $t_o$  and  $t_b$  in 10  $\mu\text{M}$  QX-222 at -125 mV, were  $3.3 \pm 3.1$  (ms) and  $4.6 \pm 4.8$  for 150 mM NaCl,  $6.8 \pm 6.3$  and  $2.2 \pm 1.8$  for mM 325 NaCl, and  $8.5 \pm 13$  and  $2.8 \pm 2.7$  for 150 mM LiCl. These results suggest that permeant ions and QX-222 compete for an intrachannel binding site, which shows higher affinity to Li than to Na. The fig. shows currents in a) 150 mM NaCl, and b) 150 mM LiCl, with 10  $\mu\text{M}$  QX at -125 mV. Scale is 50 ms and 5 pA. Supported by NS 14920.



**T-PM-Po135** DIFFERENTIATION OF THE TWO POTASSIUM CHANNELS IN CLONAL ANTERIOR PITUITARY CELLS BY THE PATCH CLAMP TECHNIQUE. Brendan S. Wong and Harold Lecar, Lab. of Biophysics, NINCDS, NIH, Bethesda, MD 20205 and Michael Adler\*, Lab. of Preclinical Studies, NIAAA, Rockville, MD 20852.

Single  $K^+$  channels were studied in intact and excised inside-out membrane patches from the anterior pituitary clone AtT-20/D16-16. Two distinct  $K^+$ -selective channels with single channel conductances differing by a factor of approximately four were observed. For both channels, opening frequencies and lifetimes depended on membrane potential. However, activation and dwell times for the channel with the larger unitary conductance were also dependent on the free  $Ca^{2+}$  concentration bathing the inner membrane surface, while the channel with the smaller unitary conductance was essentially independent of internal  $Ca^{2+}$ . The rates of activation of the  $Ca^{2+}$ -dependent  $K^+$  channels and their open times varied nonlinearly between  $10^{-8}$  to  $10^{-6}M$  free  $Ca^{2+}$ , suggesting cooperativity or multiple binding in the gating process. The single channel conductance in excised patches with symmetrical  $K^+$  (140 mM) was estimated to be 210 pS and 52 pS for the  $Ca^{2+}$ - and voltage-dependent  $K^+$  channels respectively. In the membrane potential range studied, the  $Ca^{2+}$ -dependent  $K^+$  channel conductance is consistent with the independence principle for patches bathed in different internal and external  $K^+$  concentrations. In excised patches bathed in symmetrical  $K^+$  (140 mM), both classes of channels opened more frequently and remained open for longer periods with increasing positive potentials. However, in some patches, similar increases in activation frequencies and channel open times were also observed with increasing negative potentials. Addition of tetraethylammonium (20 mM) to the cytoplasmic surface led to a reversible block of the  $Ca^{2+}$ -dependent  $K^+$  channels but caused increased flickering in the voltage-dependent  $K^+$  channels.

**T-PM-Po136** THE CONFORMATION OF THE  $H^+$ -ATPase PROTEOLIPID CHANNEL IN PHOSPHOLIPID VESICLES: A CIRCULAR DICHROISM STUDY. David Mao and B.A. Wallace, Dept. of Biochemistry, Columbia University, New York, N.Y. 10032.

The mitochondrial proton-ATPase proteolipid from *Neurospora crassa* was incorporated into small unilamellar dimyristoyl phosphatidylcholine vesicles by several different methods which preserve its activity. Circular dichroism spectroscopy (CD) indicated the secondary structure of proteolipid in vesicles is largely  $\alpha$ -helical with possibly a single beta turn. The best fit to the data was for helical segments of length  $\approx 26$  residues. This is consistent with a helical hairpin type structure in which 2 helices spanning the membrane are joined by a beta turn in the external loop, with small amounts of random coils at the N and C termini. In organic solvents and detergents, the helix is also the predominant structural motif for this protein, however, the proportions and types of other secondary structures present are significantly different, suggesting a different structure is formed in these solvents than in vesicles. No significant changes in channel conformation were observed upon binding of the  $H^+$ -ATPase inhibitor of dicyclohexylcarbodiimide to the proteolipid in vesicles. Additionally very similar CD spectra were obtained for vesicles with different lipid/protein mole ratios, indicating either that there were no substantial conformational differences between monomers and multimers, or that monomers self-associate to form stable complexes during incorporation into vesicles. Thus, this study provides not only a physical basis for model building studies of the membrane protein structure, but also preliminary information concerning features important to its functional properties. Supported by NIH Grant 27292.